Supporting Information

Total hydrogenation of bio-derived furans over supported Ru subnanoclusters prepared via amino acid-assisted deposition

Yang Qian[†,§], Ze-Jun Li[†,§], Xian-Long Du[‡], Qi Zhang[†], Yi Zhao[†], Yong-Mei Liu*[,†] and Yong Cao*[,†]

[†]*Shanghai Key Laboratory of Molecular Catalysis and Innovative Materials, Department of Chemistry, Fudan University, Shanghai 200433, China*

[‡]*Shanghai Institute of Applied Physics, Chinese Academy of Sciences, Shanghai 201204, China*

[§]These two authors contribute equally to this work.

*Corresponding author; E-mail: yongcao@fudan.edu.cn; ymliu@fudan.edu.cn

1. General procedure for the synthesis of furan/acetone adducts

All the aldol adducts were prepared by previously reported methods. [S1] Typically, for the synthesis of FFR/acetone adduct, 20 mmol FFR, 1.5 g CaO and 50 mL acetone was added in a 250 mL stainless steel batch reactor. The mixture was stirred at 140 °C for 4 h under nitrogen atmosphere. The obtained liquid was purified by column chromatography using a mixture of ethyl acetate and petroleum ether (v/v = 1:10) and dried by anhydrous Na_2SO_4. All the adol adducts and their corresponding hydrogenated products were identified by ^{1}H-NMR and ^{13}C-NMR.

2. Mathematical expressions

$$\text{Conversion (\%)} = \left(1 - \frac{amount\ of\ detected\ substrate\ [mmol]}{amount\ of\ loaded\ substrate\ [mmol]}\right) \times 100$$

$$\text{Selectivity (\%)} = \frac{amount\ of\ detected\ product\ [mmol]}{\sum amount\ of\ products\ [mmol]} \times 100$$

$$\text{Yield (\%)} = \frac{amount\ of\ detected\ product\ [mmol]}{amout\ of\ loaded\ substrate\ [mmol]} \times 100$$

$$\text{TON} = \frac{amount\ of\ accumulated\ product\ [mmol]}{amount\ of\ Ru\ utilized\ [mmol]}$$

$$\text{ATOF} = \frac{amount\ of\ detected\ product\ [mmol]}{amount\ of\ Ru\ utilized\ [mmol]\ \times\ reaction\ time\ [h]}$$

$$\text{Rate of FFR or FA conversion} = -\frac{change\ in\ content\ of\ substrate\ [mmol]}{time\ interval\ [h]}$$

3. The elimination of mass transfer limitation

Based on Weisz-Prater and Mears Criterion, we verified the absence of mass transfer limitation in measurement.

3.1 Weisz-Prater Criterion for Internal Diffusion

If $N_{W-P} = \frac{-r_A \rho_b R^2}{C_{Ab} D_e} < 1$, the internal mass transfer effects can be neglected.

$$N_{W-P} = \frac{-r_A \rho_b R^2}{C_{Ab} D_e} = \frac{2.08 \times 10^{-5} \times 3 \times 10^4 \times (1.5 \times 10^{-4})^2}{520 \times 4.26 \times 10^{-9}} = 6.34 \times 10^{-3} < 1$$

Therefore, internal mass transfer limitation is proved absent.

3.2 Mears Criterion for External Diffusion

If $\frac{-r_A \rho_b Rn}{C_{Ab} k_c} < 0.15$, the external mass transfer effects can be neglected.

$$\frac{-r_A \rho_b Rn}{C_{Ab} k_c} = \frac{2.08 \times 10^{-5} \times 3 \times 10^4 \times 1.5 \times 10^{-4} \times 1}{520 \times 6.93 \times 10^{-4}} = 2.60 \times 10^{-4} < 0.15$$

Therefore, external mass transfer limitation is proved absent.

3.3 Parameters used in the Weisz-Prater criterion and Mears Criterion

Parameter	Value
Reaction rate: $-r_A (mmol/mg_{cat} \cdot s)$	2.08×10^{-5}
Density of catalyst: $\rho_b (kg/m^3)$	3×10^4
Radius of catalyst: $R\ (m)$	$1.5 \times 10^{-4} (100\ mesh)$
Surface reactant concentration: $C_{Ab} (kmol/m^3)$	520
Effective liquid-phase diffusivity: $D_e (m^2/s)$[a]	4.26×10^{-9}
Reaction order: n	1
Mass transfer coefficient: $k_c (m/s)$[b]	6.93×10^{-4}
Viscosity of ethanol: $\eta_{EtOH} (Pa \cdot s)$	3.32×10^{-4}
Latent heat of vaporization of ethanol: $L_{EtOH}\ (J/kmol)$	3.94×10^7

Latent heat of vaporization of FFA: $L_{FFA}\ (J/kmol)$	4.28×10^{7}
Schmidt number: Sc[c]	1512
Reynolds number: Re[d]	1102
Sherwood number: Sh[e]	231
Viscosity of the reactant mixture: $\mu\ (Pa \cdot s)$	1.074×10^{-3}
Density of reactant mixture: $\rho\ (kg/m^3)$	789
Liquid-phase diffusivity: $D_{Ab}(m^2/s)$	9×10^{-10}
Superficial velocity: $U\ (m/s)$	10

a $D_e = 4.4 \times 10^{-15} \frac{T}{\eta_{EtOH}} \left(\frac{V_{EtOH}}{V_{FFA}}\right)^{1/6} \left(\frac{L_{EtOH}}{L_{FFA}}\right)^{1/2}$

b $k_c = \frac{ShD_{Ab}}{2R}$

c $Sc = \frac{\mu}{\rho D_{Ab}}$

d $Re = \frac{UR\rho}{\mu}$

e $Sh = 2 + 0.6Re^{1/2}Sc^{1/3}$

4. Supplementary data

Table S1. Summary of TPR results

Sample	Metal (mmol)	Peak Quantity	H_2 Consumption (mmol)	Reduction Degree[a]
Ru/TiO_2-lys-DP	4.85×10^{-3}	4.25	7.67×10^{-3}	79%
Ru/TiO_2-DP	5.54×10^{-3}	6.08	11.0×10^{-3}	99%

[a] Based on the assumption that the unreduced species are sole RuO_2. [S2]

Table S2. Summary of EXAFS fits at Ru K-edge

Sample	Coordination	CN	R(Å)	$\sigma^2(\times10^{-3}Å^2)$	ΔE(eV)	R-factor
Ru foil	Ru-Ru	12	2.67	--	--	--
Ru/TiO_2-lys-DP	Ru-O	5.2	1.96	7.7	-3.1	1.39%
	Ru-Ru	1.5	2.66	5.4	-3.1	
Ru/TiO_2-DP	Ru-O	2.7	1.91	5.7	-5.7	0.72%

	Ru-Ru	4.9	2.67	5.1	-5.7	
RuO_2	Ru-O	6	1.98	--	--	--

CN, coordination number; R, distance between absorber and backscatter atoms; σ^2, Debye-Waller factor.

Table S3. Catalytic activities of recently reported heterogeneous and homogeneous catalysts for total hydrogenation of FFR

Catalyst	S/C	Temp. (°C)	H_2 (MPa)	Time (h)	ATOF(h^{-1})	Ref.
Ru/TiO_2-lys-DP	550	80	4	1.5	367	This work
Ru/TiO_2-lys-DP	550	2	4	25	22	This work
Pd-Ir/SiO_2	89	2	8	4	21	S3
Ni-Pd/SiO_2	33	40	8	2	17	S4
Ni-Pd/TiO_2-ZrO_2	66	130	5	8	8	S5
Pd/Al_2O_3	11	90	2	2	4	S6
Pd/Al_2O_3	220	25	6	8	27	S7
Pd/MFI	350	220	3.4	5	67	S8
Pd/HAP	368	40	1	4	92	S9
Pd-Pt/TiO_2	500	30	0.3	4	119	S10
Ru/ZrO_2+Pd/Al_2O_3	45	30	0.5	3	12	S11
CuNi/CNT	14	130	4	10	1	S12
CuNi/MgAlO	12	150	4	3	4	S13
Ni-Ba/Al_2O_3	15	140	4	4	4	S14
Ni/C	12	120	1	2	6	S15
Ni/NAC	6	80	4	3	2	S16
Ru@C/TiO_2	290	80	4	7	41	S17
Ru@G-CS	20	180	3	2	10	S18
polyCTR-β-CD Ru	50	30	1	4	7	S19

S/C, the molar ratio of substrate to active metal.

ATOF, average turnover frequency (based on maximum product yield)

Table S4. Effect of solvent on FFR hydrogenation

Entry[a]	Solvent	Conv. (%)	Selectivity (%)[b]		
			THFA	FA	Others[c]
1	MeOH	>99	57	37	6
2	EtOH	>99	>99	0	0
3	2-propanol	>99	31	69	0
4	THFA	>99	11	89	0
5	THF	70	3	86	11
6	DMF	30	0	83	17
7	toluene	27	0	>99	0
8	*n*-heptane	44	0	>99	0
9	H_2O	81	2	98	0
10[d]	THFA	>99	>99	0	0

[a] Reaction conditions: FFR (5.2 mmol), solvent (10 mL), Ru/TiO_2-lys-DP (metal 0.18 mol%), H_2 (4 MPa), 80 °C, 1.5 h. [b] Determined by GC methods using naphthalene as internal standard. [c] Others include ethers and unidentified oligomers. [d] 4 h.

Table S5. Summary of the XPS results of Ru/TiO_2-lys-DP reduced at different temperatures

Reduction temperature (°C)	Ratio between species (%)	
	$Ru^{\delta+}/(Ru^0+Ru^{\delta+})$	$Ti^{3+}/(Ti^{3+}+Ti^{4+})$
100	50	10
300	20	40
500	5	50

Table S6. Summary of the XPS results of Ru/TiO_2-DP reduced at different temperatures

Reduction temperature (°C)	Ratio between species (%)	
	$Ru^{\delta+}/(Ru^0+Ru^{\delta+})$	$Ti^{3+}/(Ti^{3+}+Ti^{4+})$
100	20	0
300	0	0
500	0	20

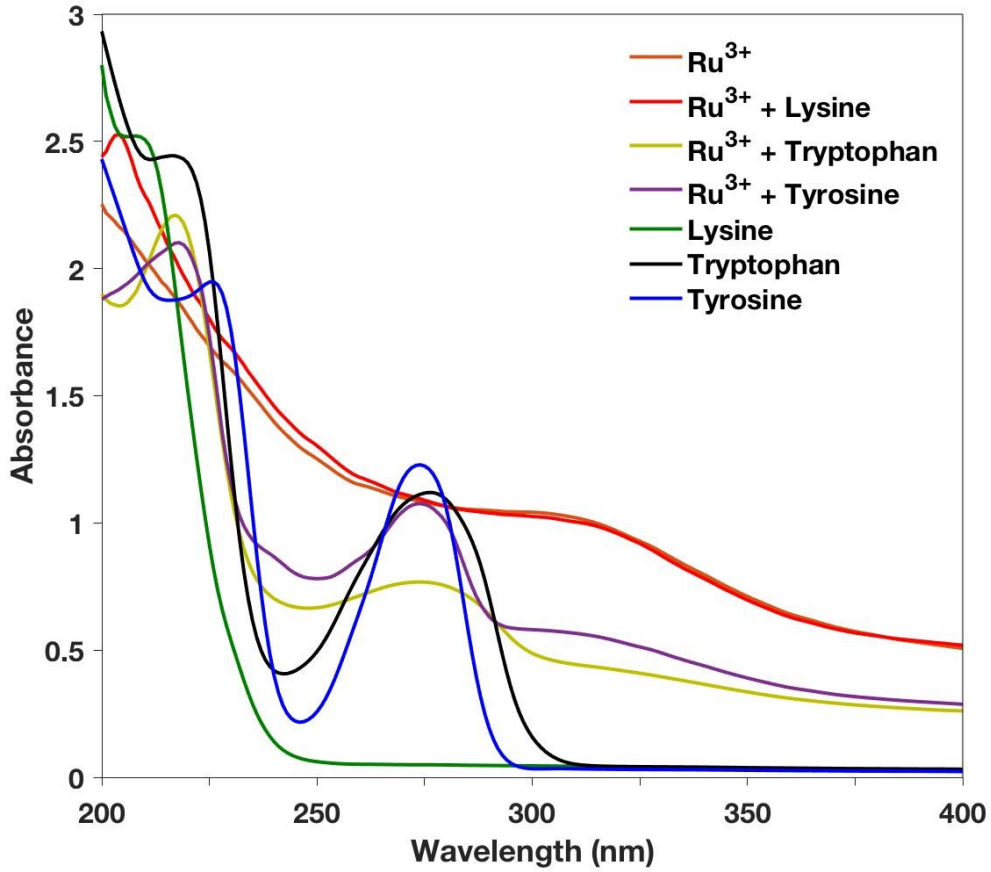

Fig. S1 UV-vis spectra of aqueous solutions containing various species

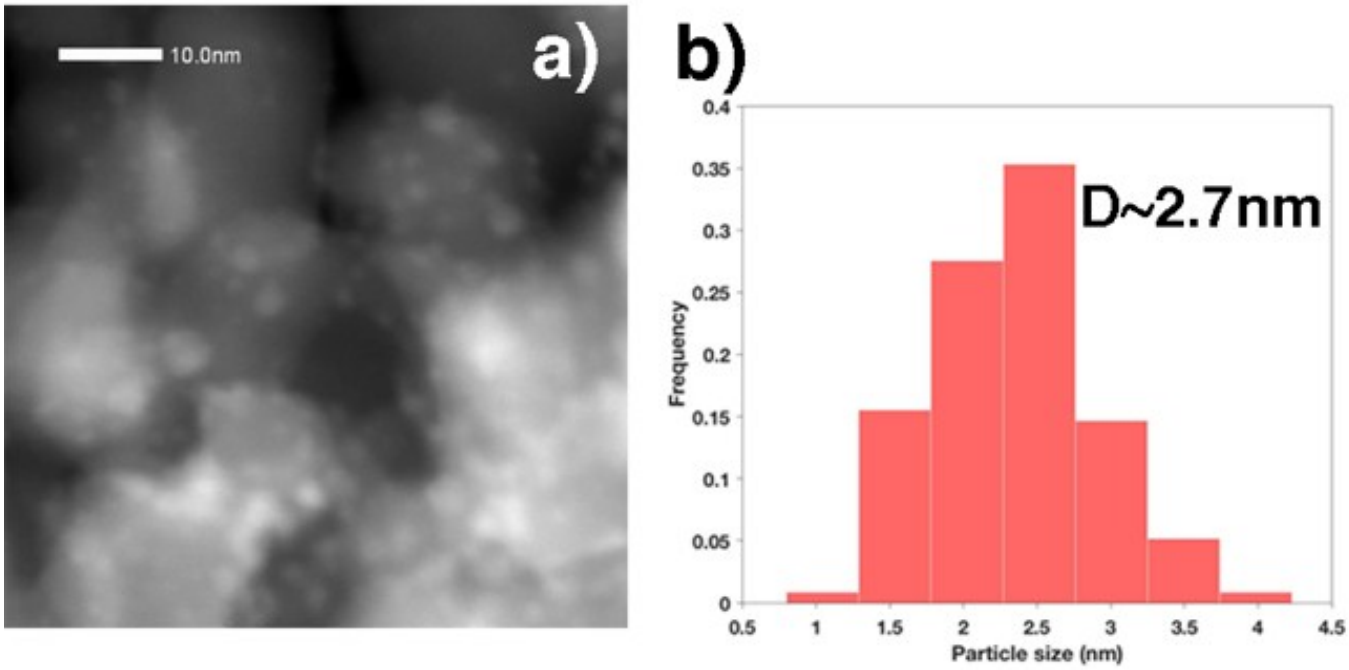

Fig. S2 HAADF-STEM image (a) and corresponding particle size distribution (b) of Ru/TiO_2-DP

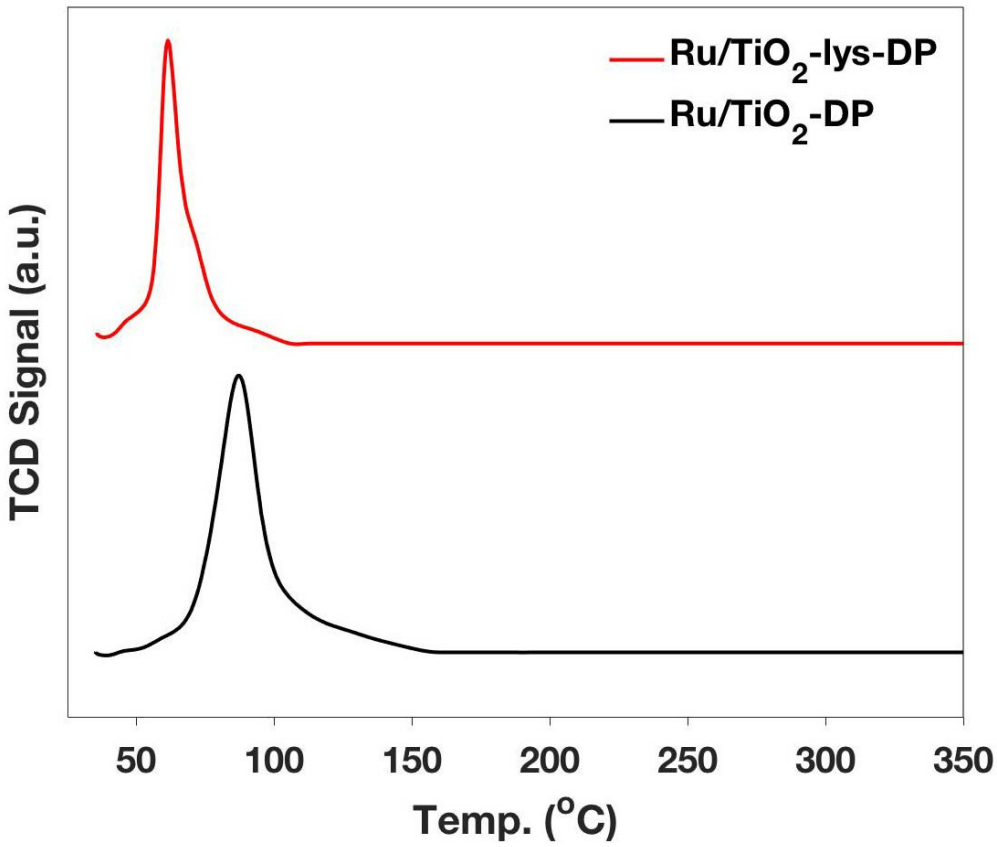

Fig. S3 TPR profiles of Ru/TiO_2-lys-DP and Ru/TiO_2-DP

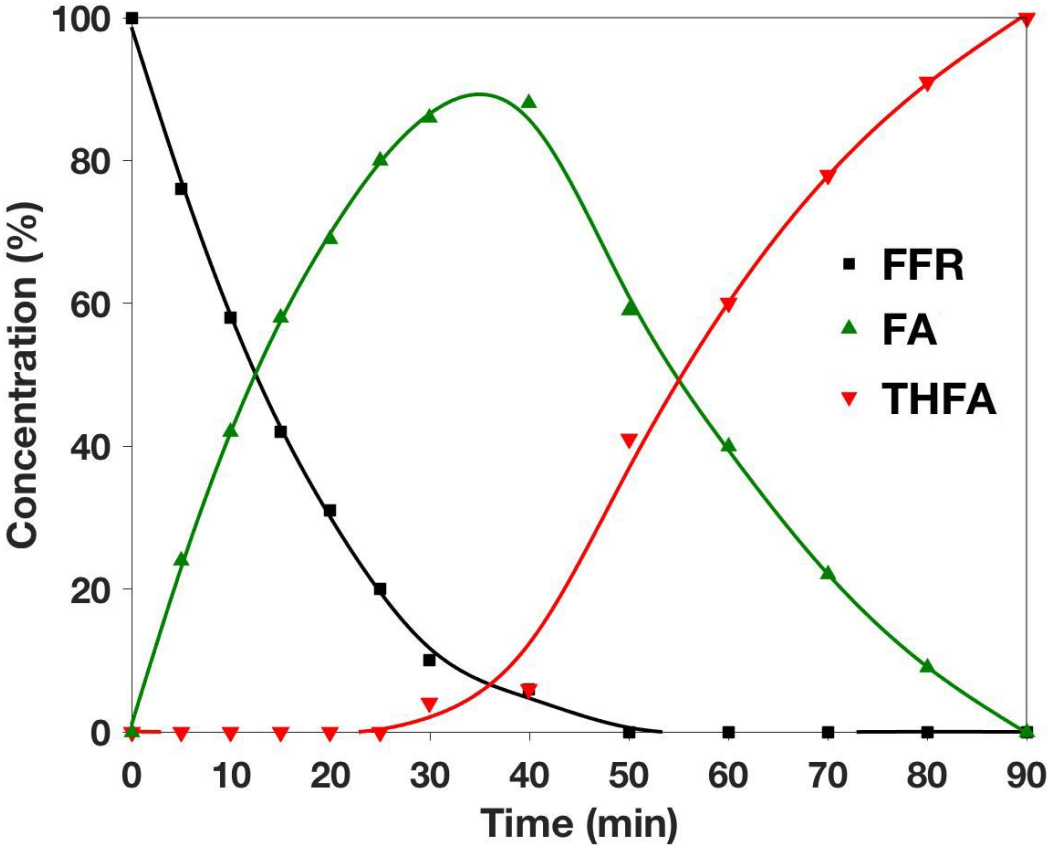

Fig. S4 Reaction profile of Ru/TiO_2-lys-DP in FFR hydrogenation. Reaction conditions: FFR (5.2 mmol), EtOH (10 mL), catalyst (metal 0.18 mol%), H_2 (4 MPa), 80 °C.

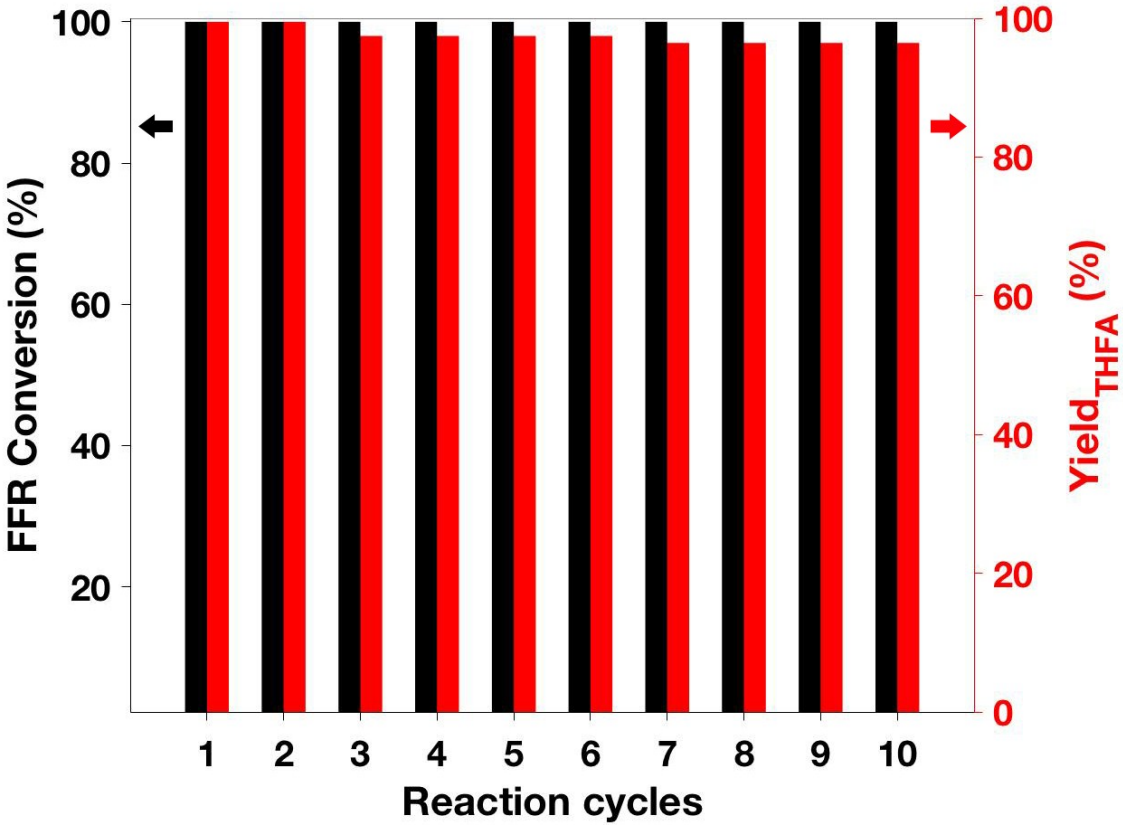

Fig. S5 Reuse of Ru/TiO_2-lys-DP in 5.2mmol-scale hydrogenation of FFR. Reaction conditions: FFR (5.2 mmol), EtOH (10 mL), catalyst (metal 0.18 mol%), H_2 (4 MPa), 80 °C, 1.5 h. Note: The catalysts lost about 25 wt% mass in total in repetitive recovery process.

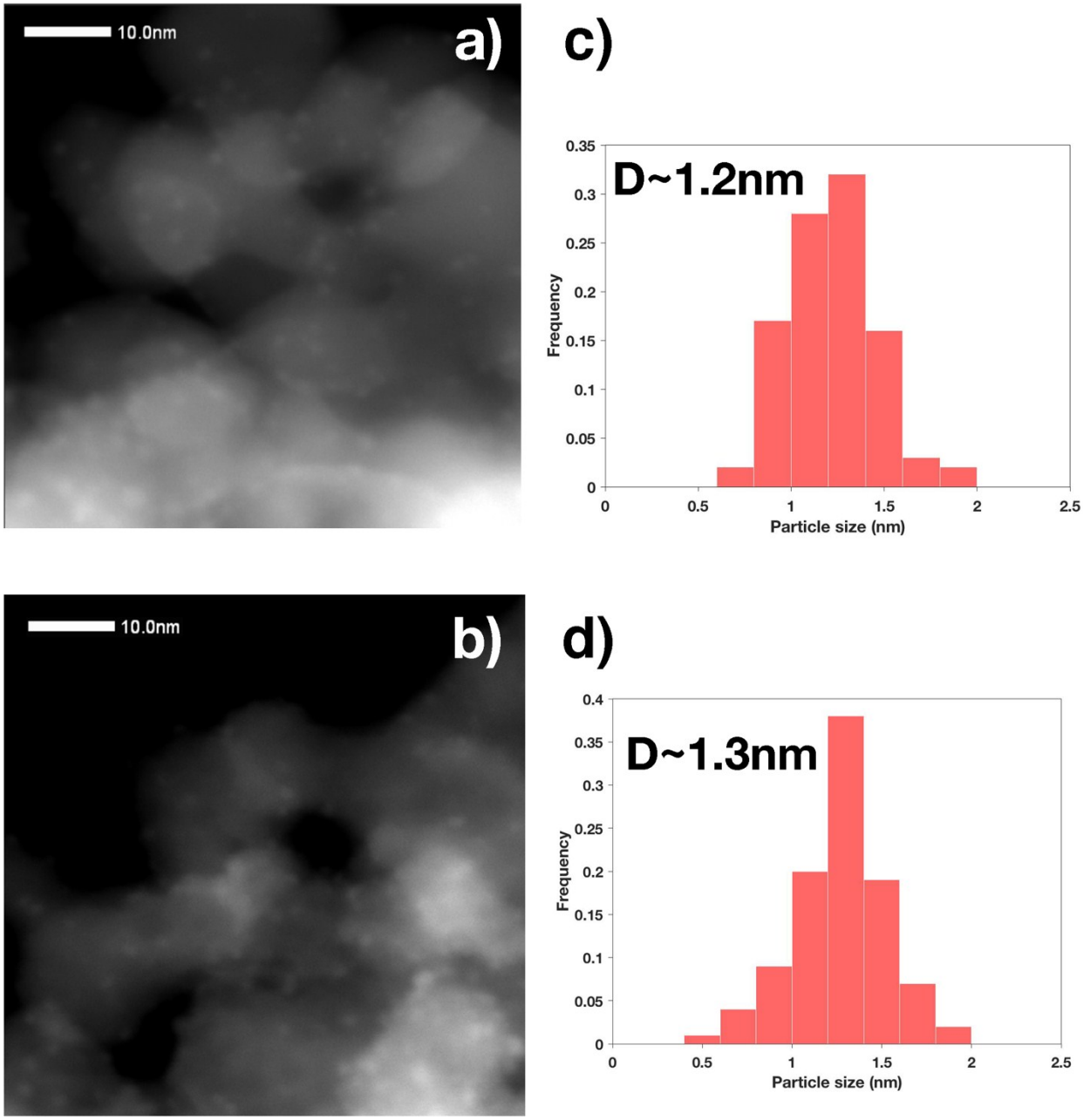

Fig. S6 HAADF-STEM images and corresponding particle size distributions of (a,c) Ru/TiO_2-trp-DP and (b,d) Ru/TiO_2-tyr-DP

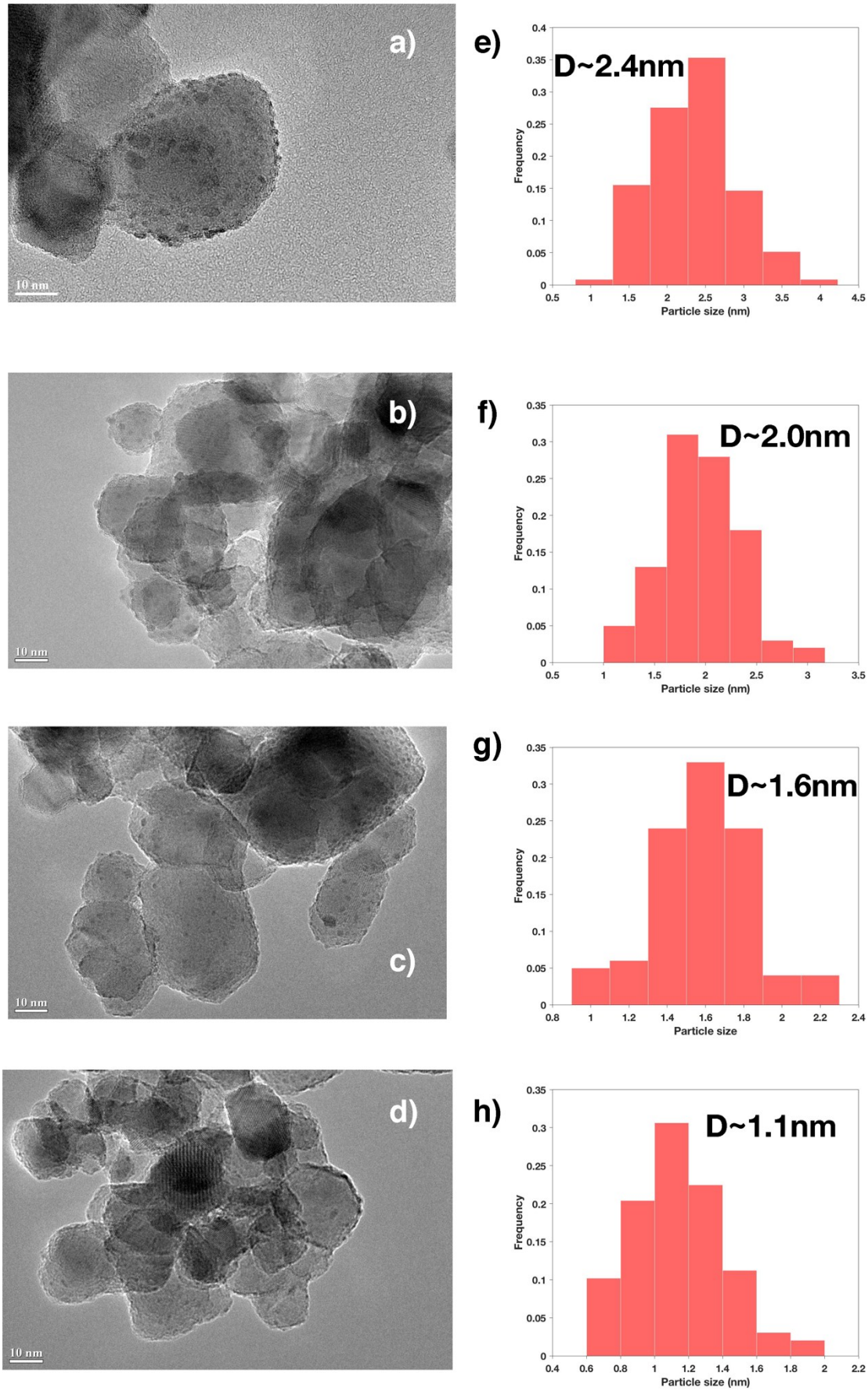

Fig. S7 TEM images and corresponding particle size distributions of Ru/TiO_2-DP catalysts prepared with (a,e) 0.01 mmol, (b,f) 0.025 mmol (c,g) 0.05 mmol and (d,h) 0.2 mmol lysine

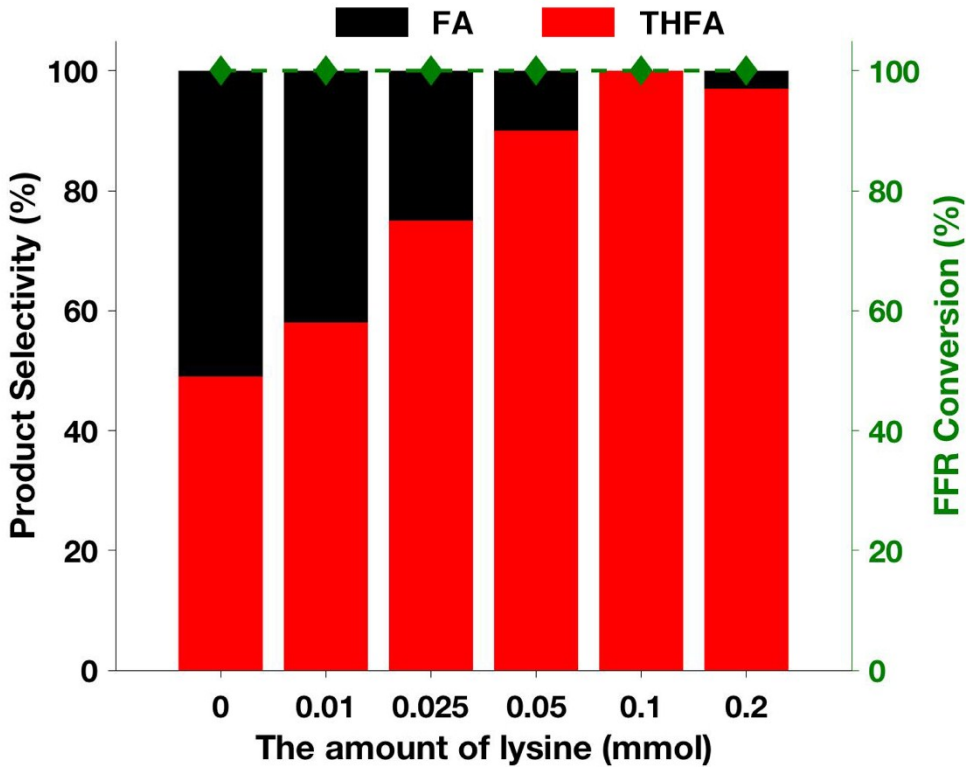

Fig. S8 Catalytic activities of Ru/TiO_2-DP catalysts prepared with various amounts of lysine in total hydrogenation of FFR. Reaction conditions: FFR (5.2 mmol), EtOH (10 mL), catalysts (metal 0.18 mol%), H_2 (4 MPa), 80 °C, 1.5 h.

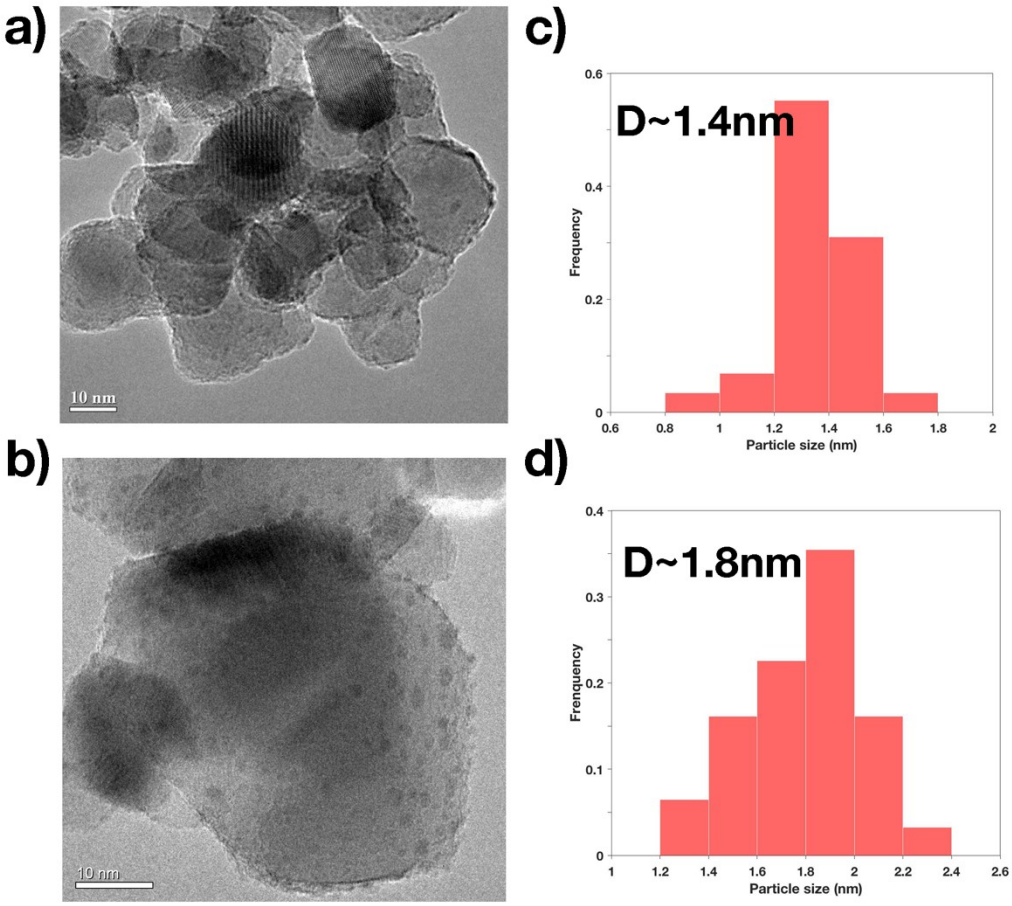

Fig. S9 TEM images and corresponding particle size distributions of (a,c) Ru/TiO_2-lys-imp and (b,d) Ru/TiO_2-imp

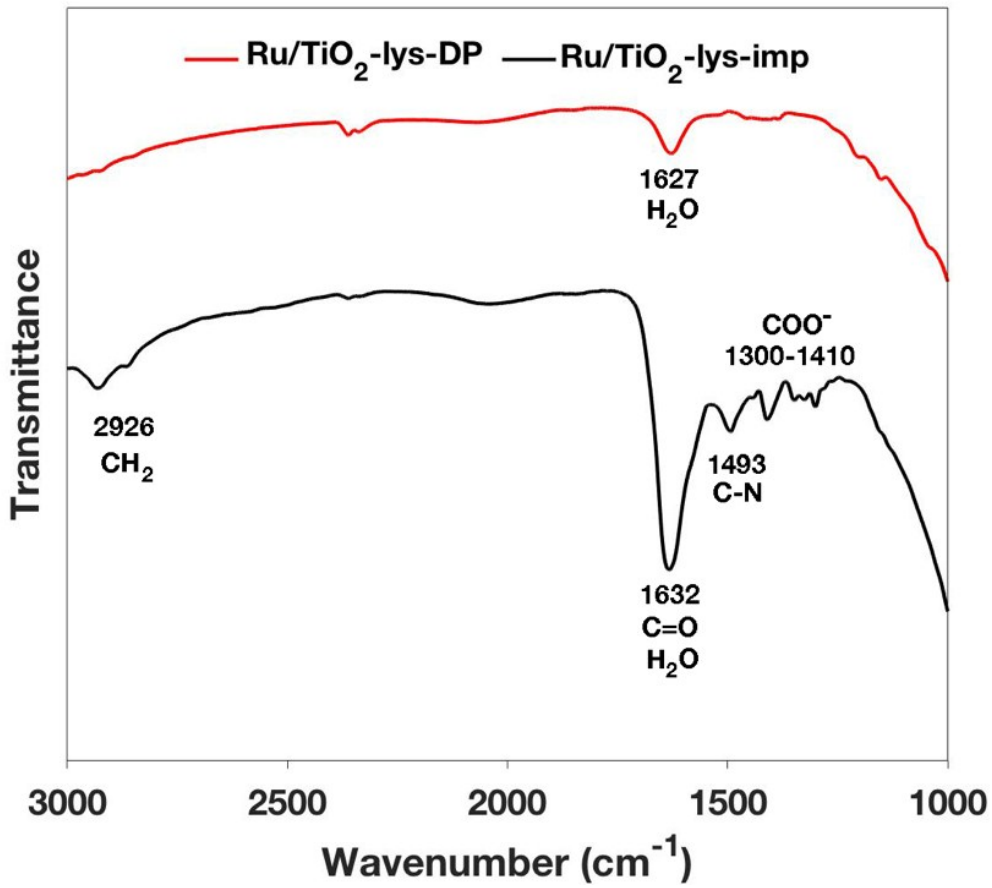

Fig. S10 FTIR spectra of Ru/TiO_2-lys-DP and Ru/TiO_2-lys-imp

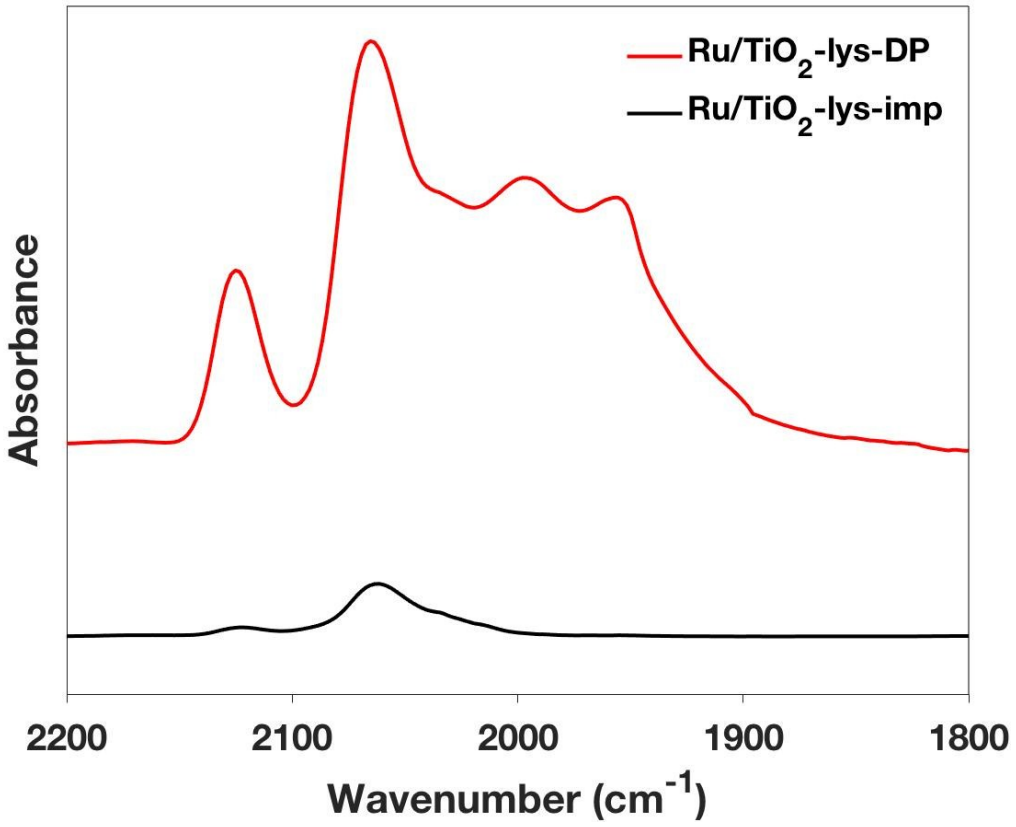

Fig. S11 DRIFT spectra in the carbonyl region of Ru/TiO_2-lys-DP and Ru/TiO_2-lys-imp

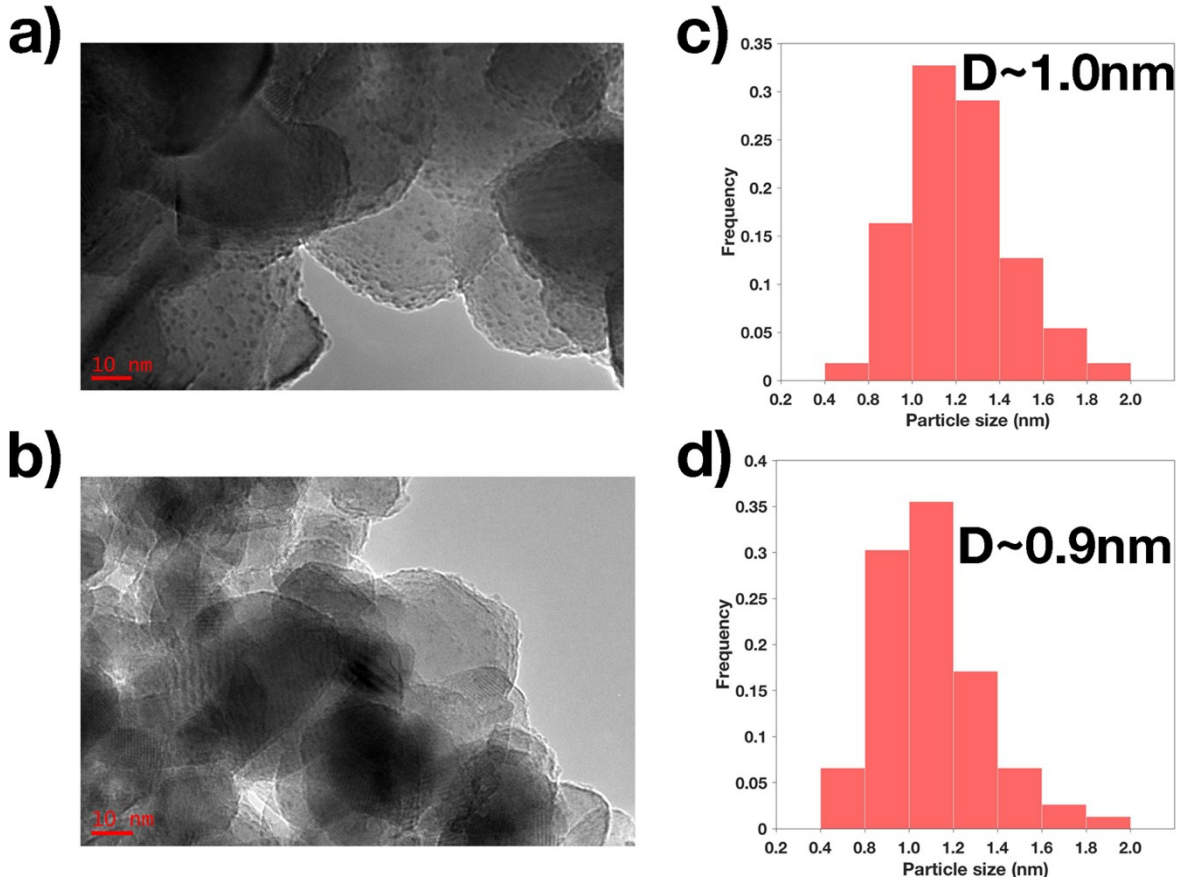

Fig. S12 TEM images and corresponding particle size distributions of (a,c) Ru/TiO_2-R-lys-DP and (b,d) Ru/TiO_2-A-lys-DP

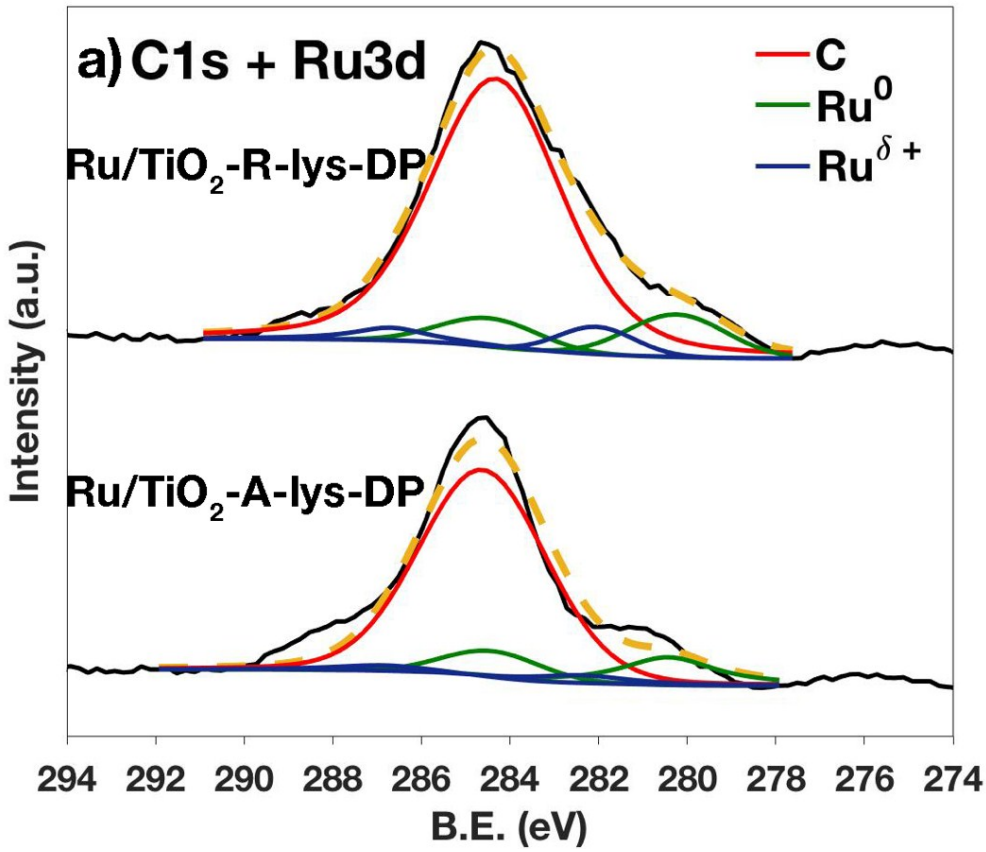

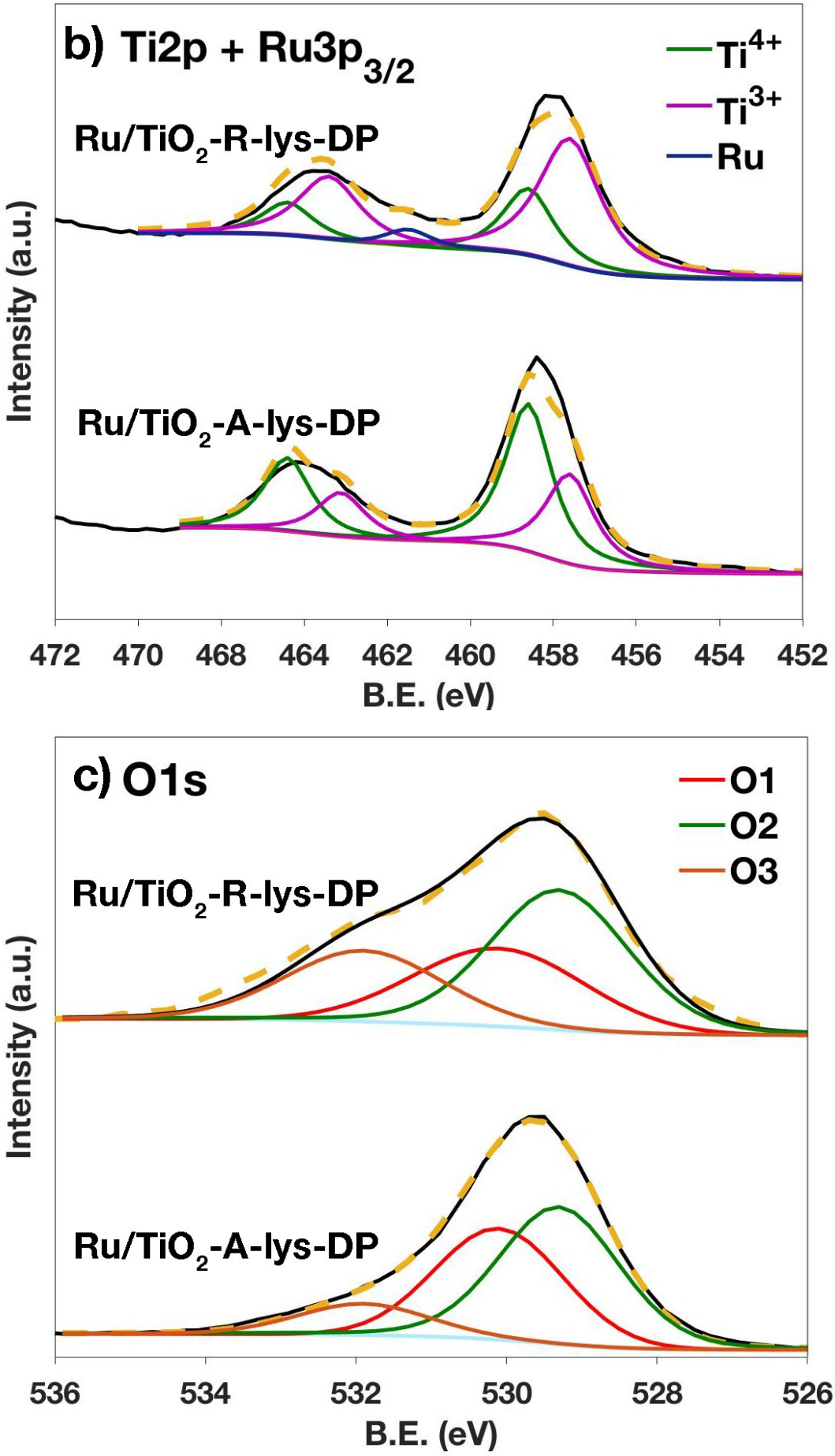

Fig. S13 XPS spectra of Ru/TiO_2-R-lys-DP and Ru/TiO_2-A-lys-DP (a) C 1s and Ru 3d spectra, (b) Ti 2p and Ru $3p_{3/2}$ spectra and (c) O 1s spectra (O1 refers to stoichiometric O in TiO_2, O2 to O in reduced TiO_x and O3 to organic and hydroxylic O) [S20]

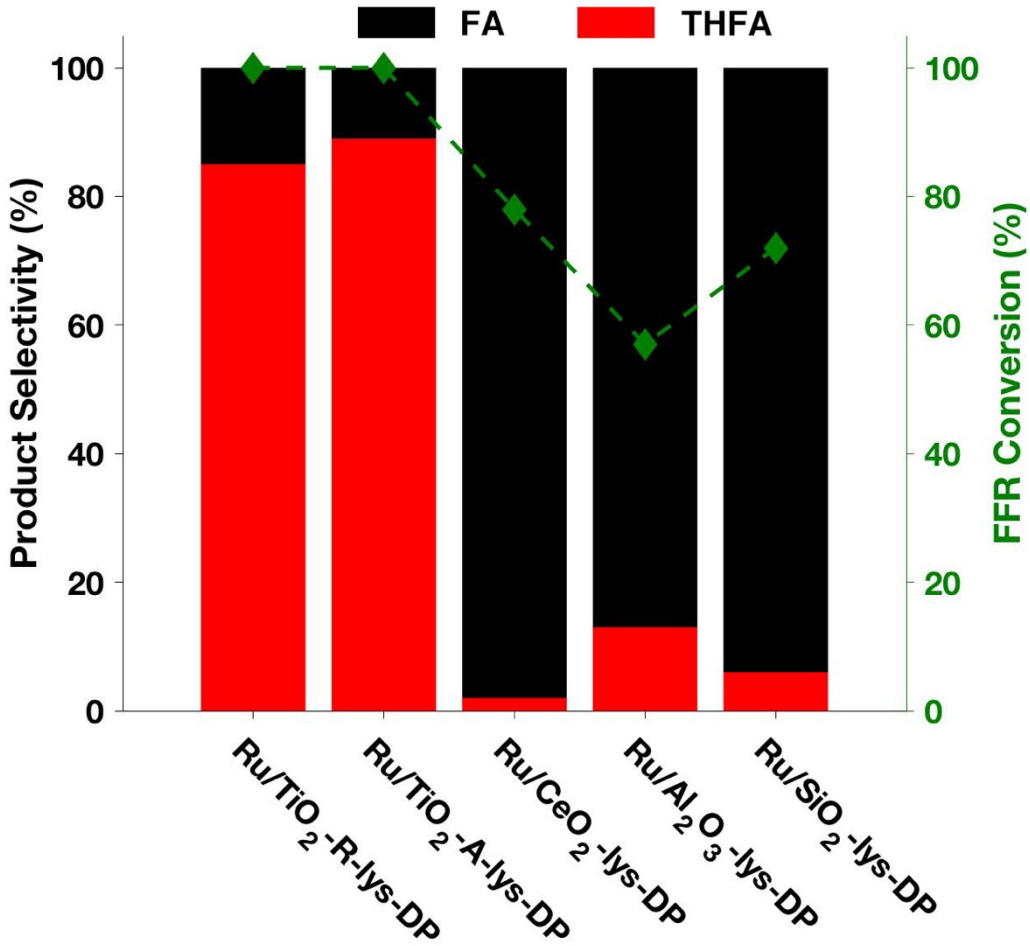

Fig. S14 Catalytic activities of Ru/MO_x-lys-DP catalysts in total hydrogenation of FFR. Reaction conditions:

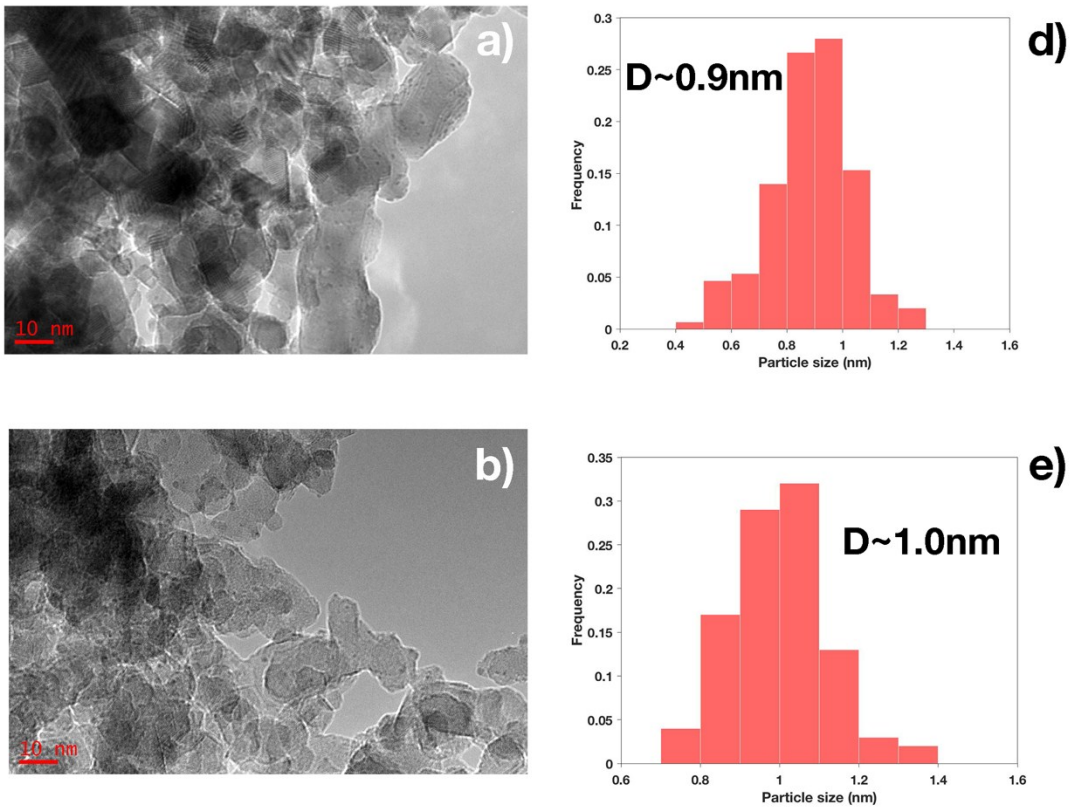

FFR (5.2 mmol), EtOH (10 mL), catalysts (metal 0.18 mol%), H_2 (4 MPa), 80 °C, 1.5 h.

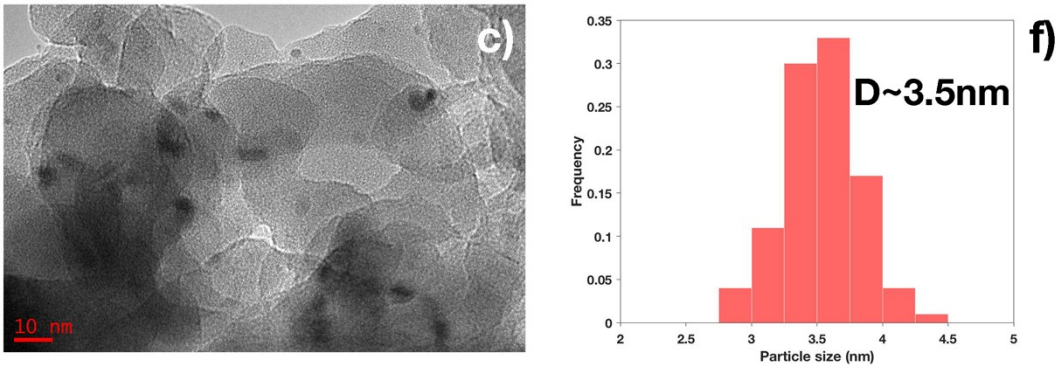

Fig. S15 TEM images and corresponding particle size distributions of (a,d) Ru/CeO_2-lys-DP, (b,e) Ru/Al_2O_3-lys-DP and (c,f) Ru/SiO_2-lys-DP

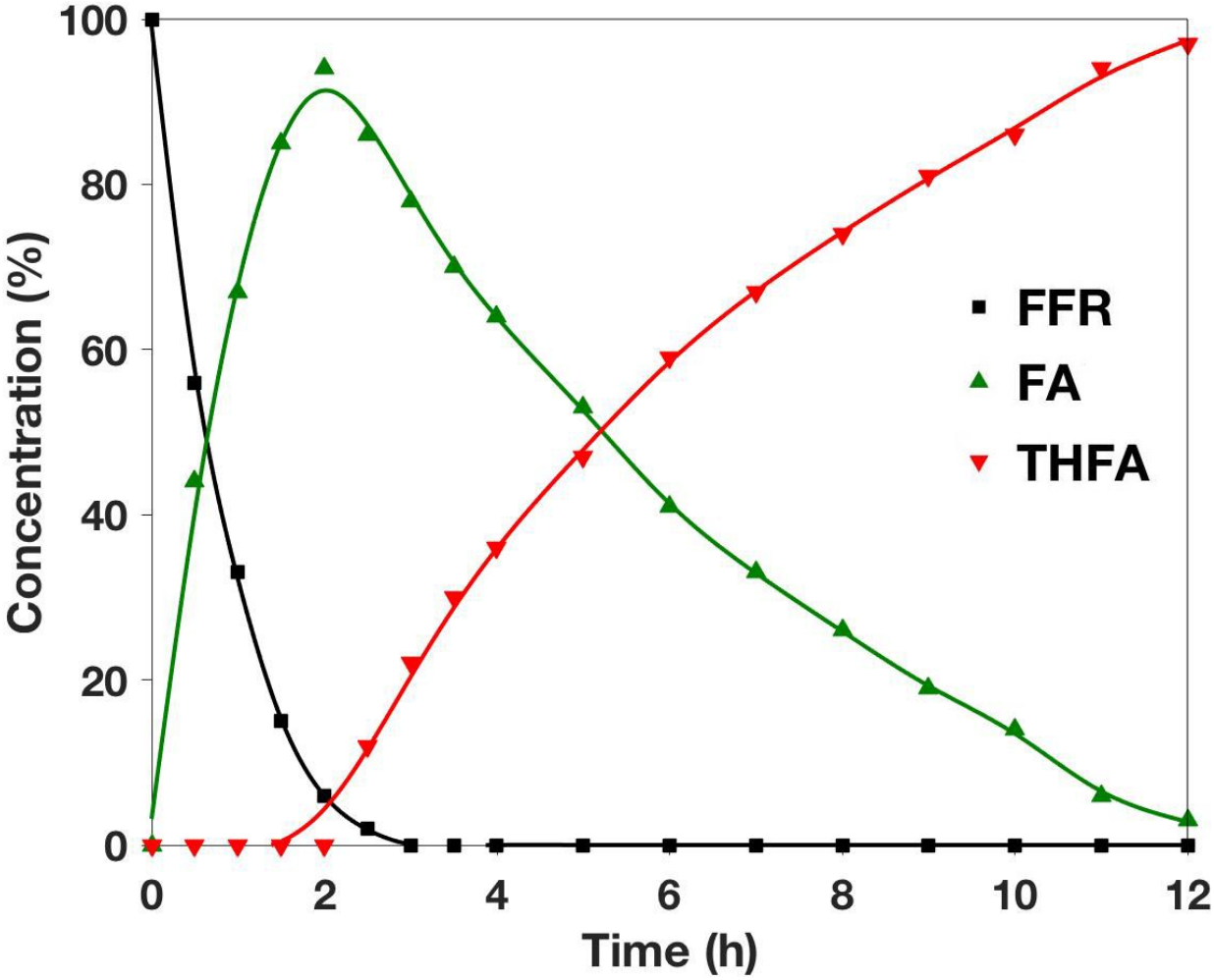

Fig. S16 Reaction profile of Ru/TiO_2-lys-DP in FFR hydrogenation. Reaction conditions: FFR (52 mmol), EtOH (10 mL), catalyst (metal 0.04 mol%), H_2 (4 MPa), 80 °C.

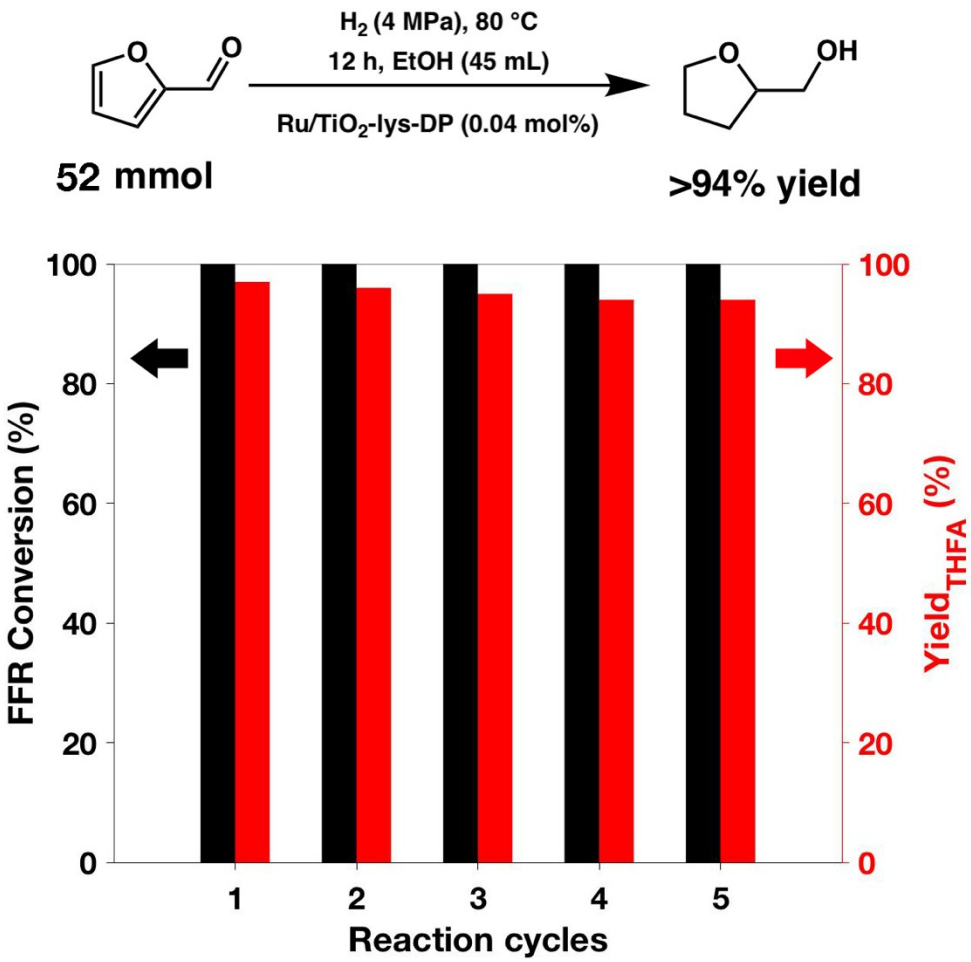

Fig. S17 Reuse of Ru/TiO_2-lys-DP in 5.2mmol-scale hydrogenation of FFR.

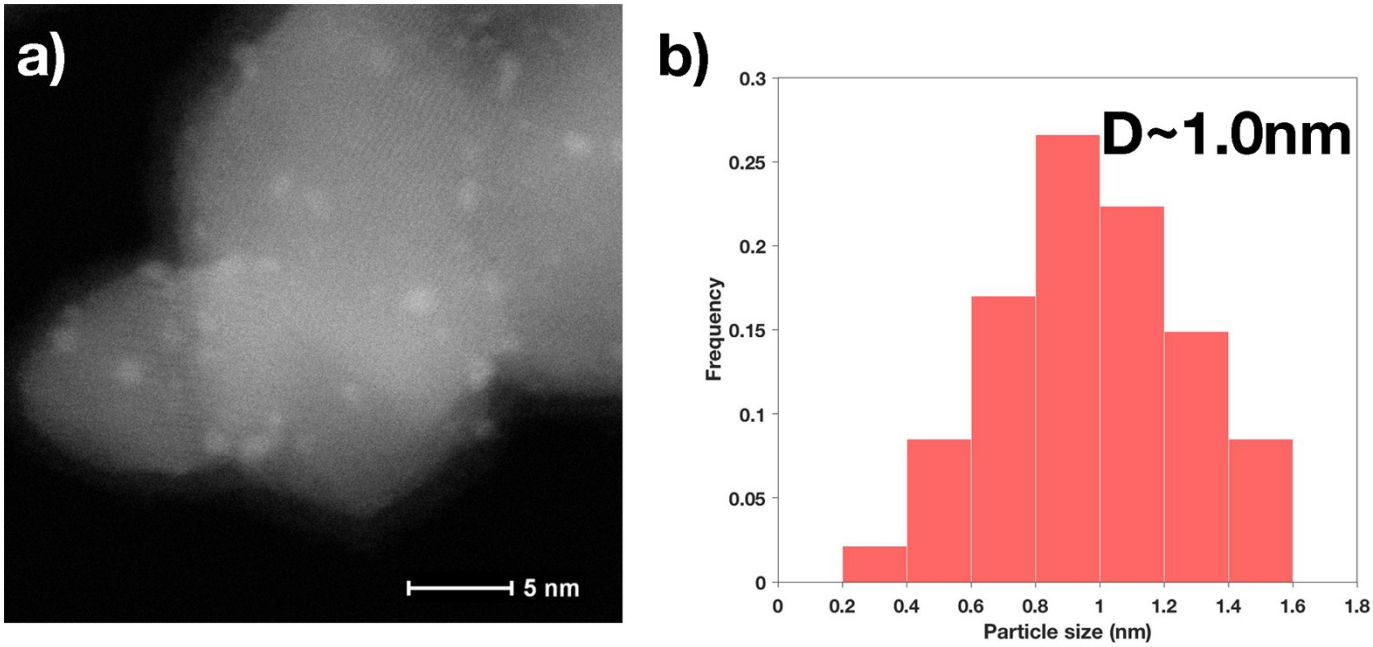

Fig. S18 HAADF-STEM image (a) and corresponding particle size distribution (b) of spent Ru/TiO_2-lys-DP

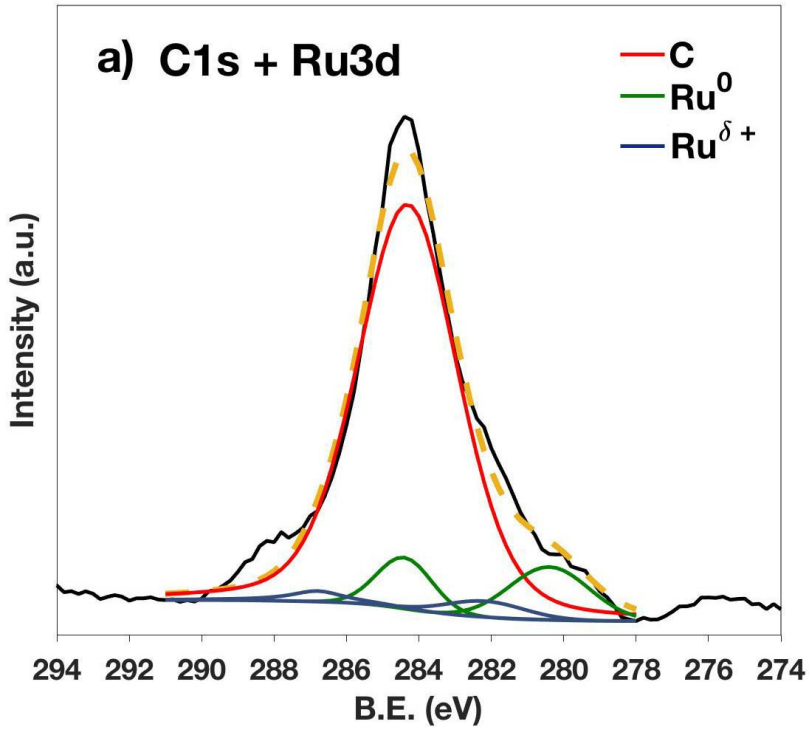
a) C1s + Ru3d
C
Ru0
Ruδ +
Intensity (a.u.)
294 292 290 288 286 284 282 280 278 276 274
B.E. (eV)

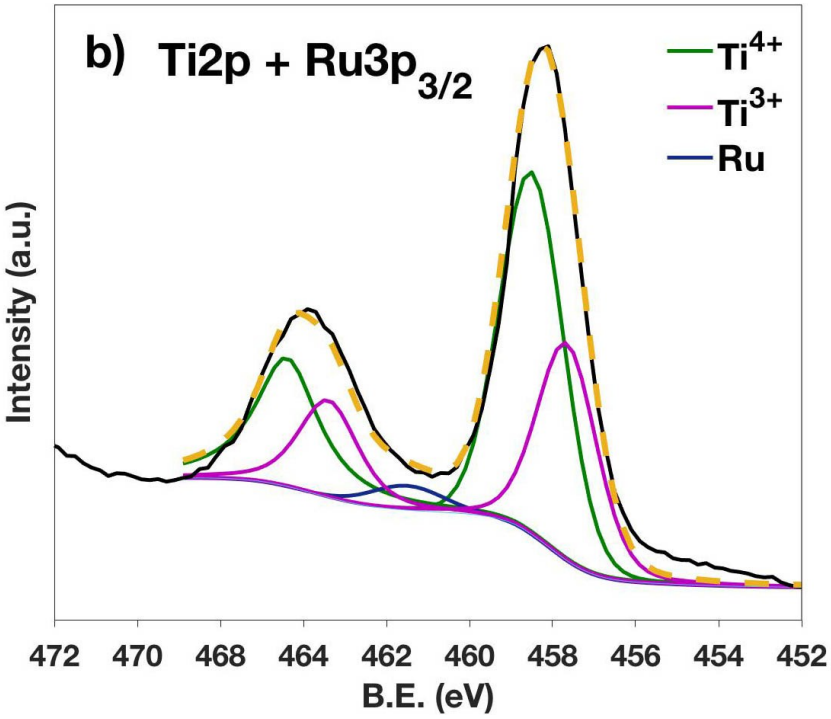
b) Ti2p + Ru3p3/2
Ti4+
Ti3+
Ru
Intensity (a.u.)
472 470 468 464 462 460 458 456 454 452
B.E. (eV)

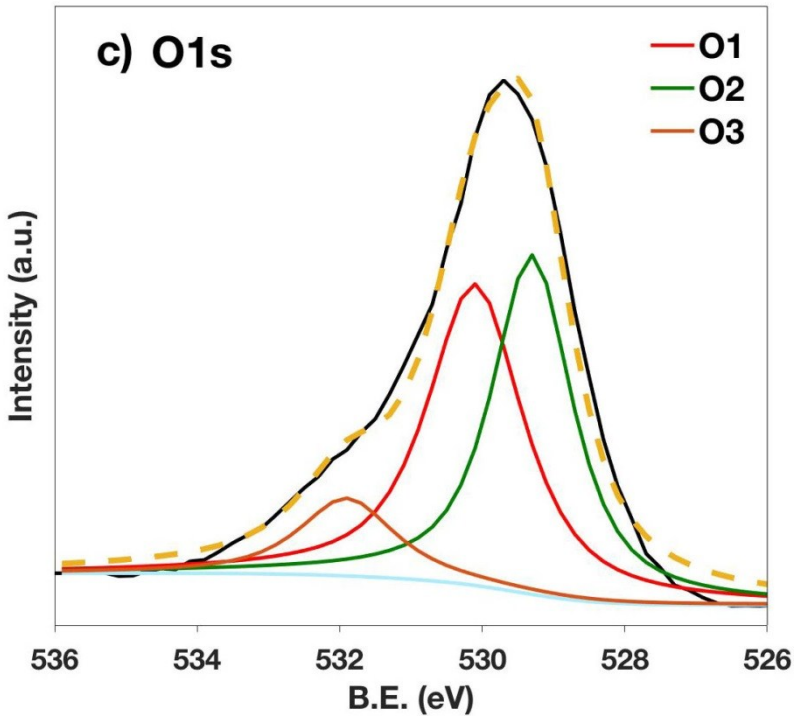

Fig. S19 XPS spectra of spent Ru/TiO_2-lys-DP (a) C 1s and Ru 3d spectra, (b) Ti 2p and Ru $3p_{3/2}$ spectra and (c) O 1s spectra (O1 refers to stoichiometric O in TiO_2, O2 to O in reduced TiO_x and O3 to organic and hydroxylic O) [S20]

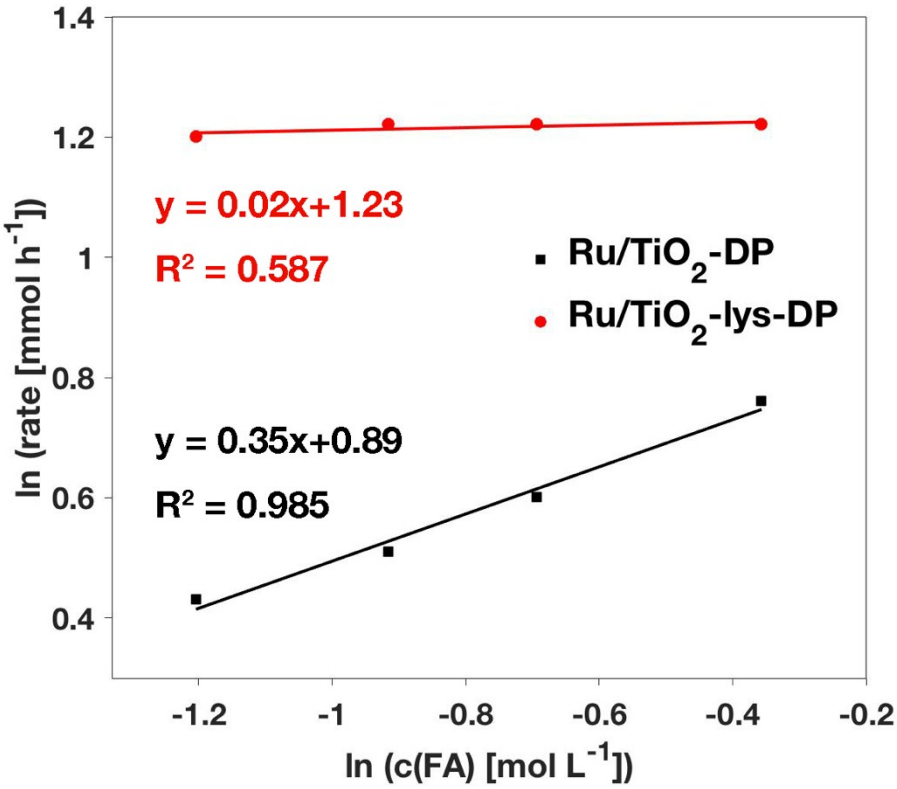

Fig. S20 Effect of FA concentration on the reaction rate. Reaction conditions: FA (3-7 mmol), EtOH (10 mL), catalysts (200 mg), H_2 (4 MPa), 25 °C. Each rate was calculated by five data points (0, 5, 10, 15 and 20 mins). The raw data are shown in Fig. S21.

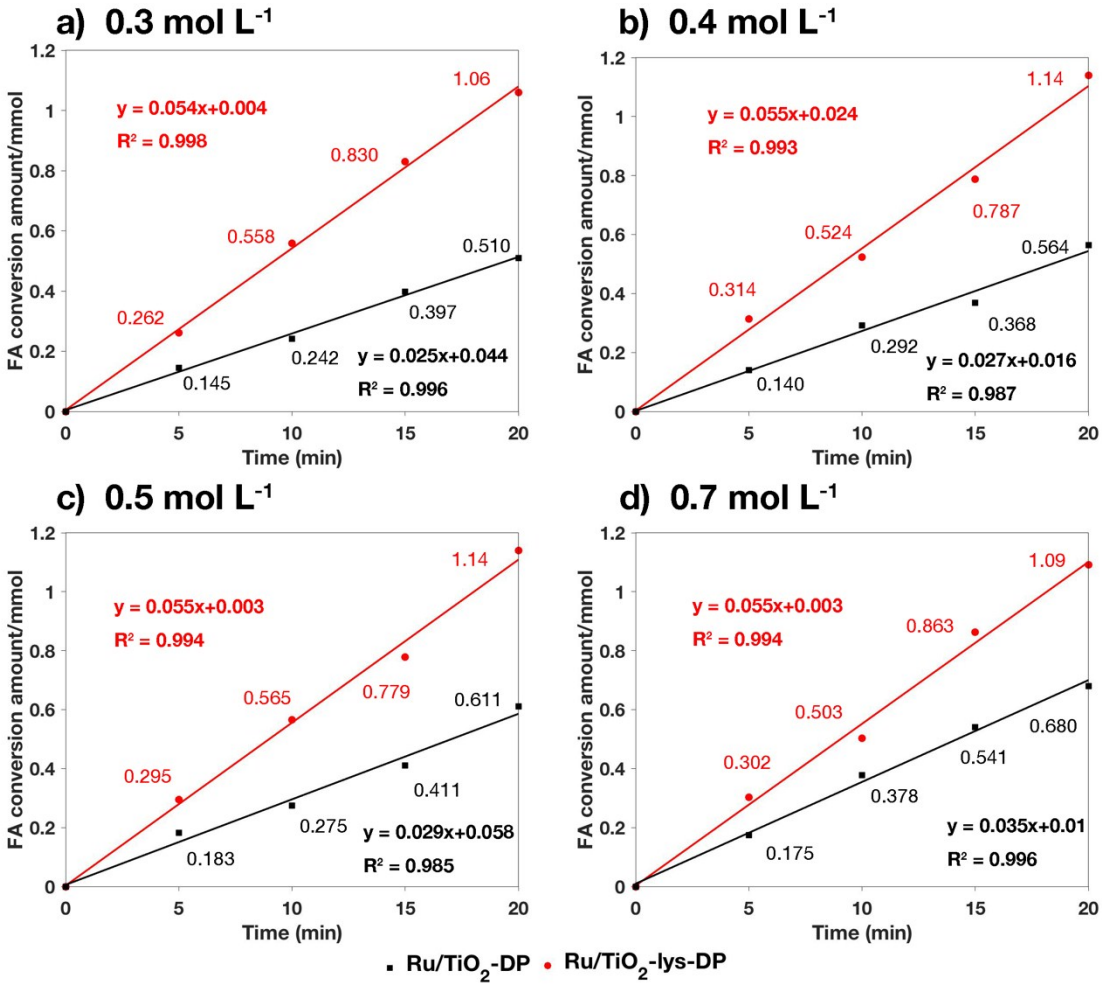

Fig. S21 Determination of FA conversion rate from the data in Fig. S20

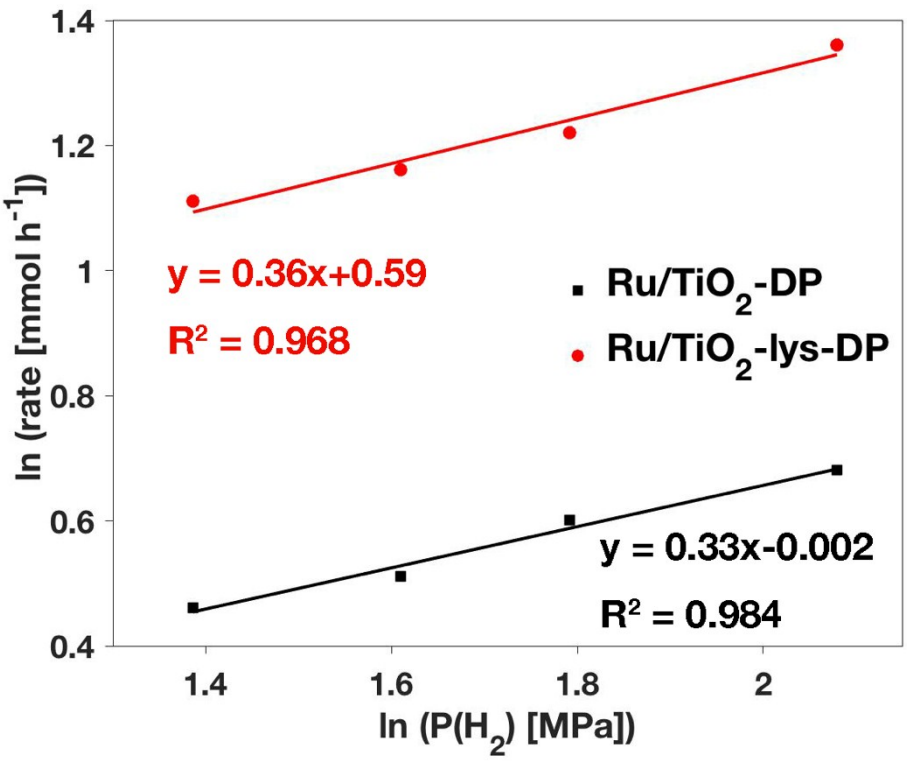

Fig. S22 Effect of H_2 pressure on the reaction rate. Reaction conditions: H_2 (4-8 MPa), FFR (5.2 mmol), EtOH (10 mL), catalysts (200 mg), 25 °C. Each rate was calculated by five data points (0, 3, 7, 10 and 15 mins). The raw data are shown in Fig. S23.

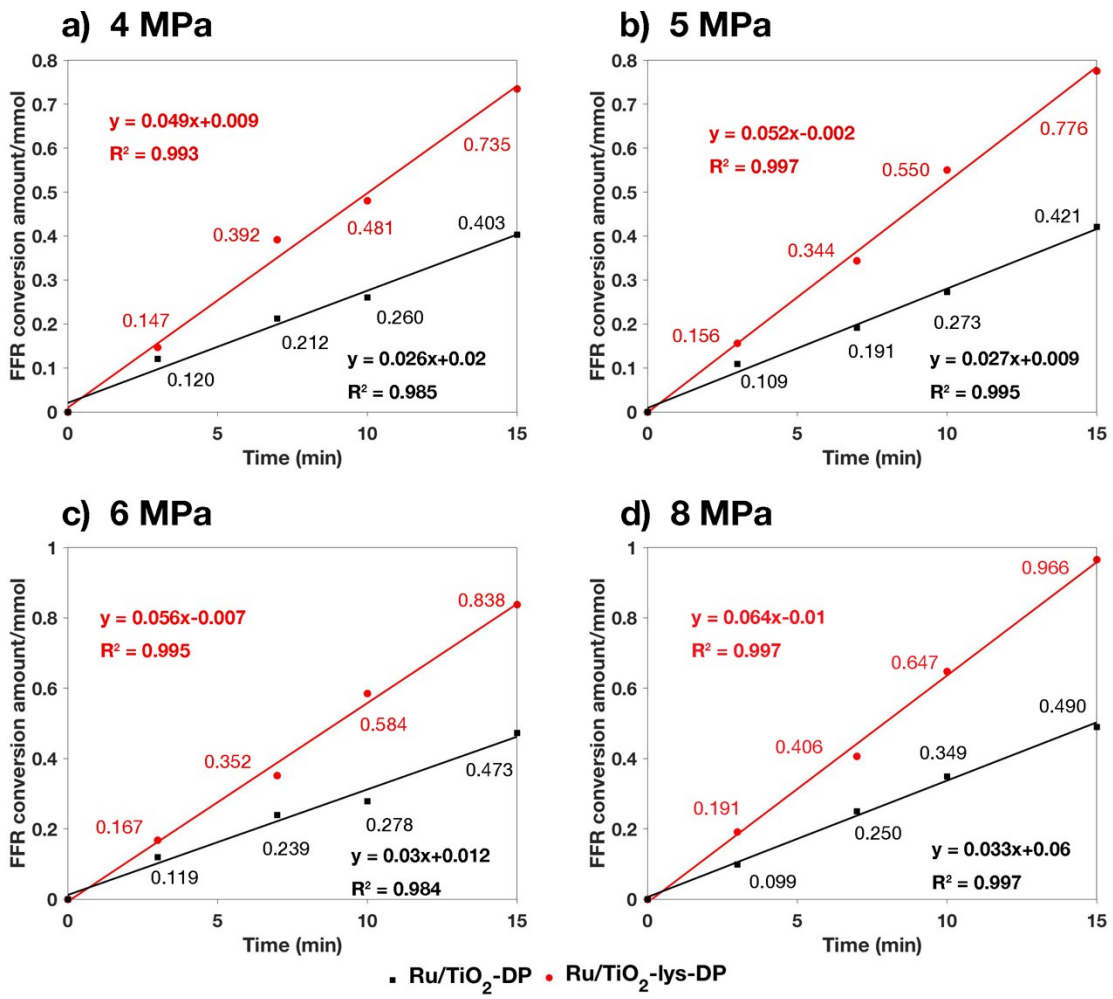

Fig. S23 Determination of FFR conversion rate from the data in Fig. S22

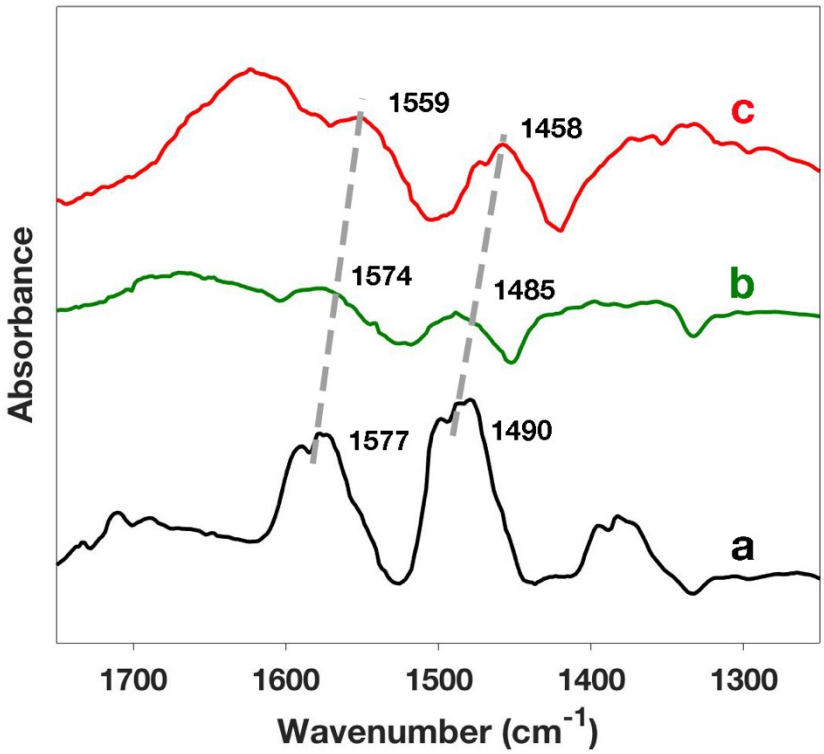

Fig. S24 *In situ* Fourier transform infrared spectra of (a) gaseous furan and furan adsorbed on (b) Ru/TiO_2-DP and (c) Ru/TiO_2-lys-DP.

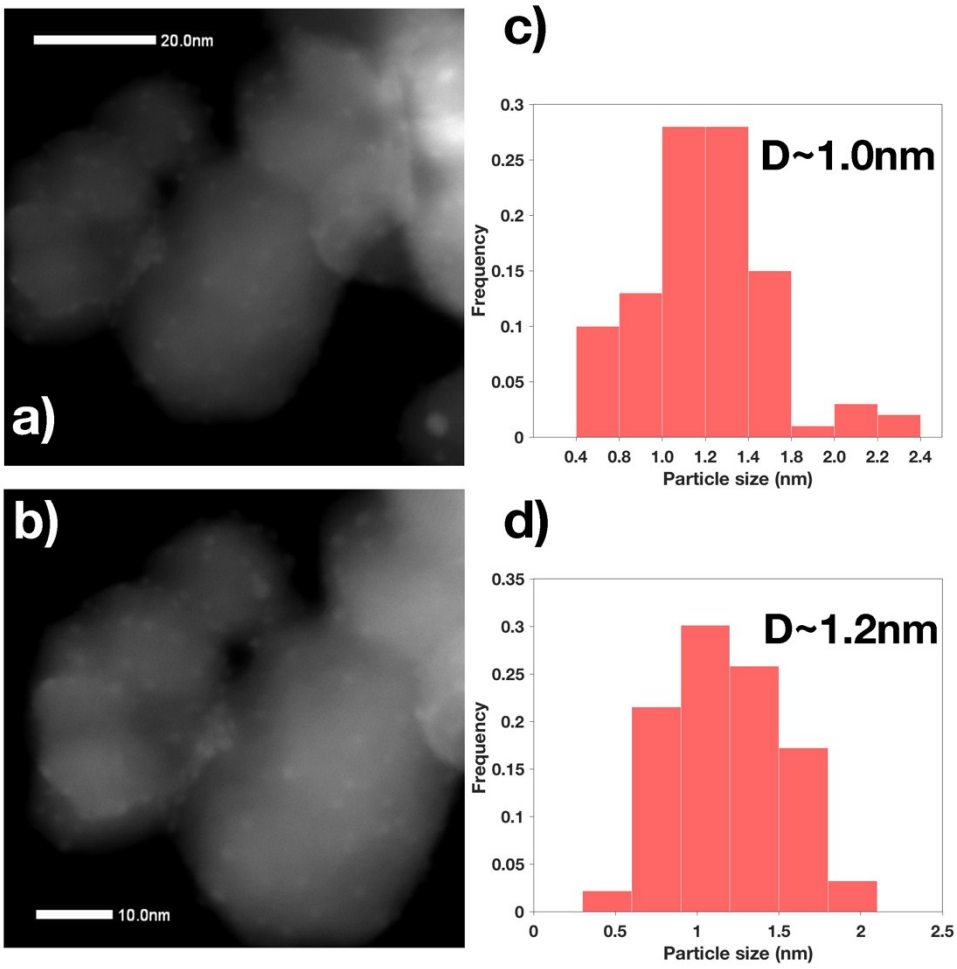

Fig. S25 HAADF-STEM images and corresponding particle size distributions of Ru/TiO_2-lys-DP reduced at

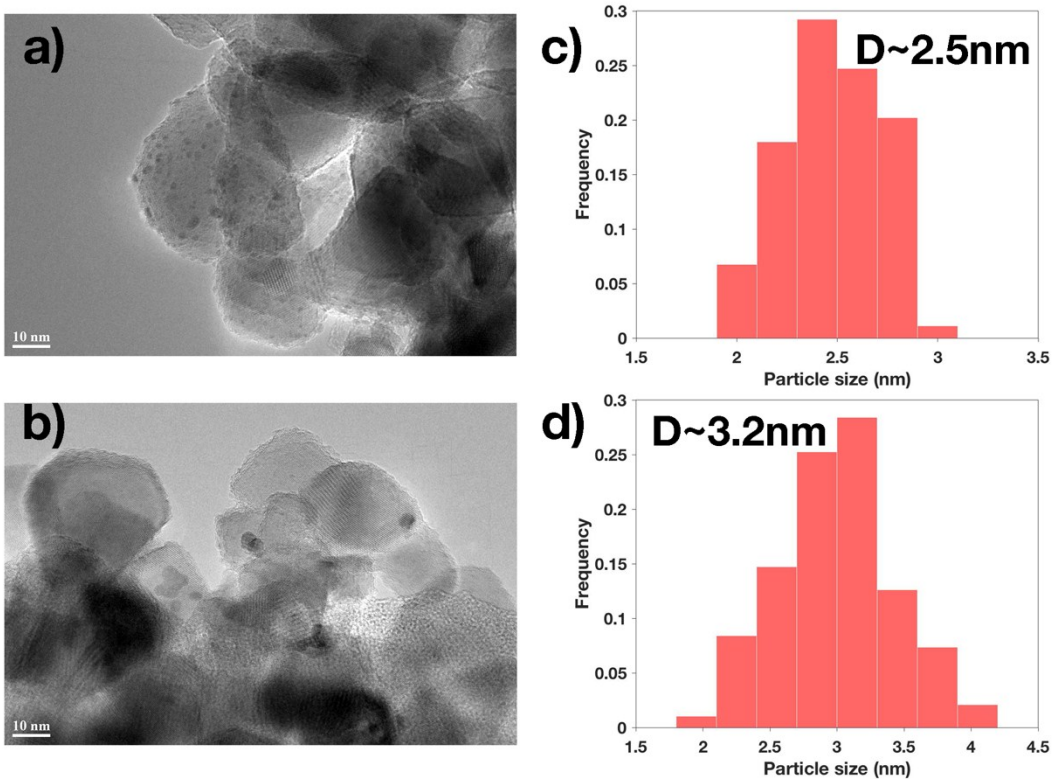

(a,c) 100 °C and (b,d) 500 °C.

Fig. S26 TEM images and corresponding particle size distributions of Ru/TiO_2-DP reduced at (a,c) 100 °C and (b,d) 500 °C

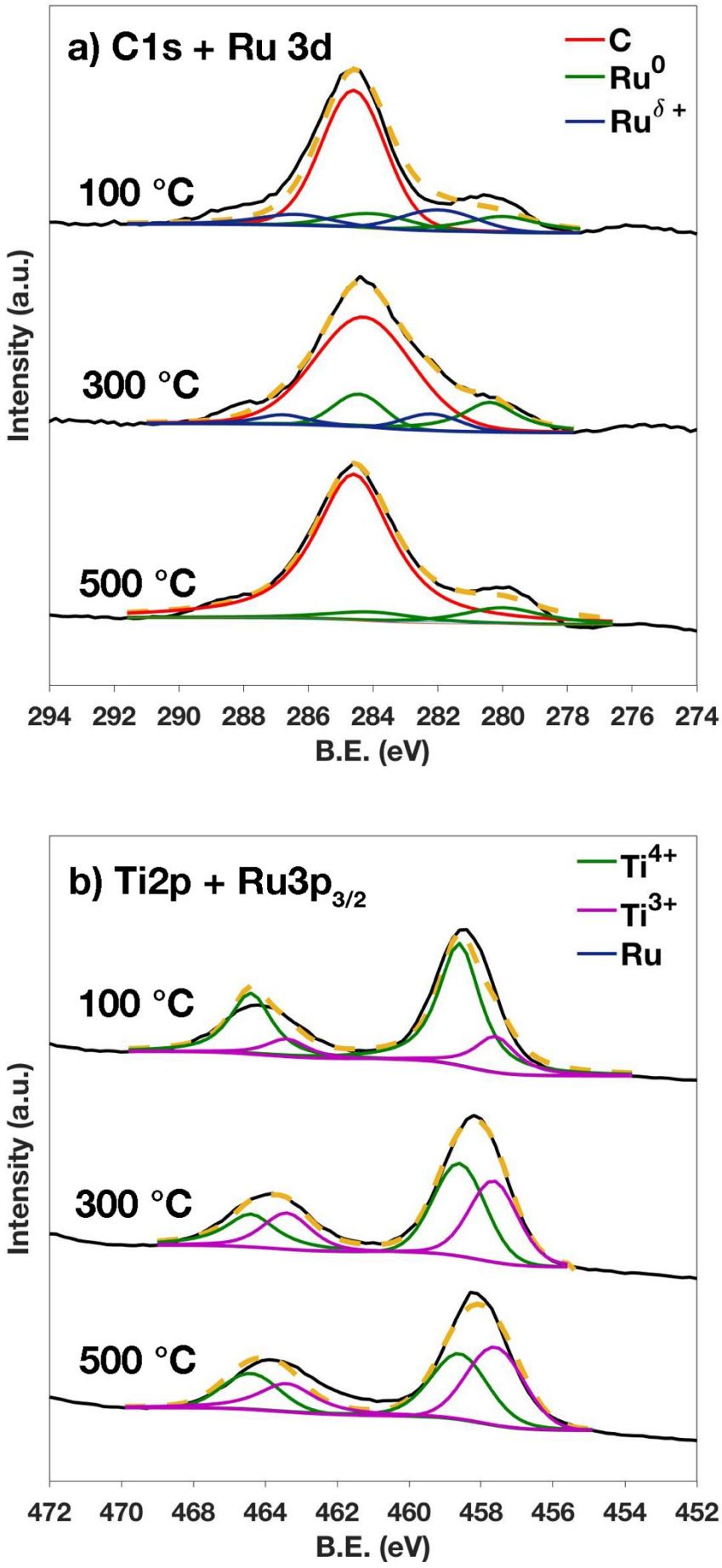

Fig. S27 XPS spectra of Ru/TiO_2-lys-DP reduced at different temperatures (a) C 1s and Ru 3d spectra and (b) Ti 2p and Ru $3p_{3/2}$ spectra. The ratios between different species are summarized in Table S5.

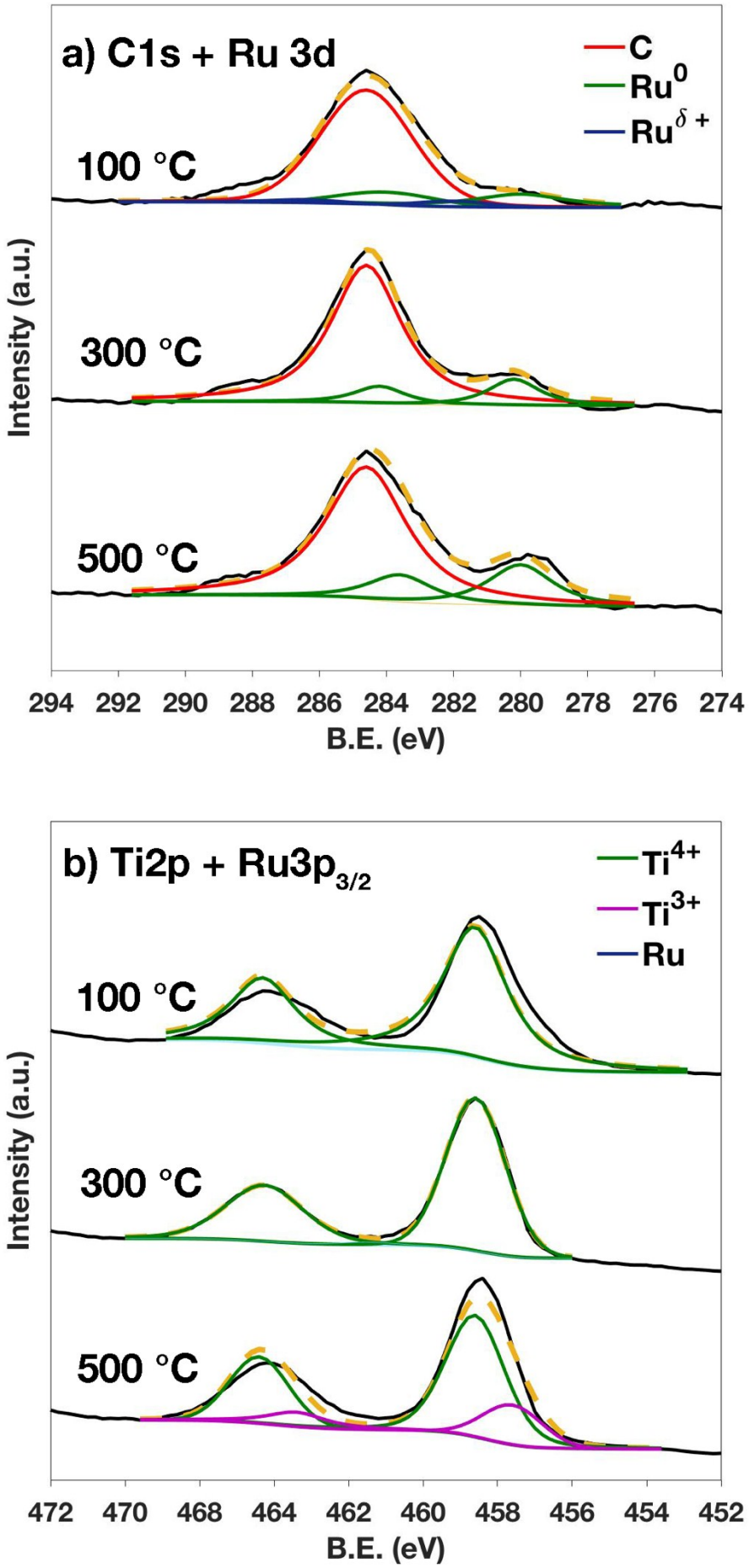

Fig. S28 XPS spectra of Ru/TiO_2-DP reduced at different temperatures (a) C 1s and Ru 3d spectra and (b) Ti 2p and Ru $3p_{3/2}$ spectra. The ratios between different species are summarized in Table S6.

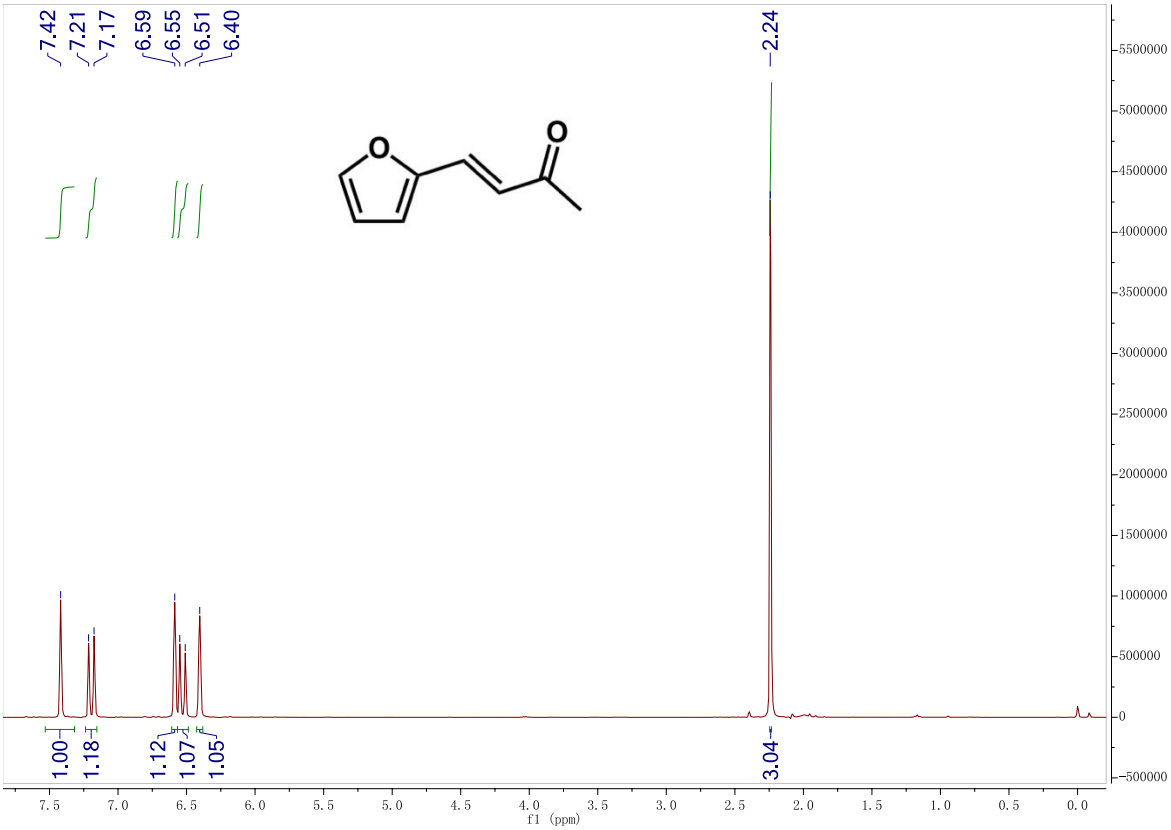

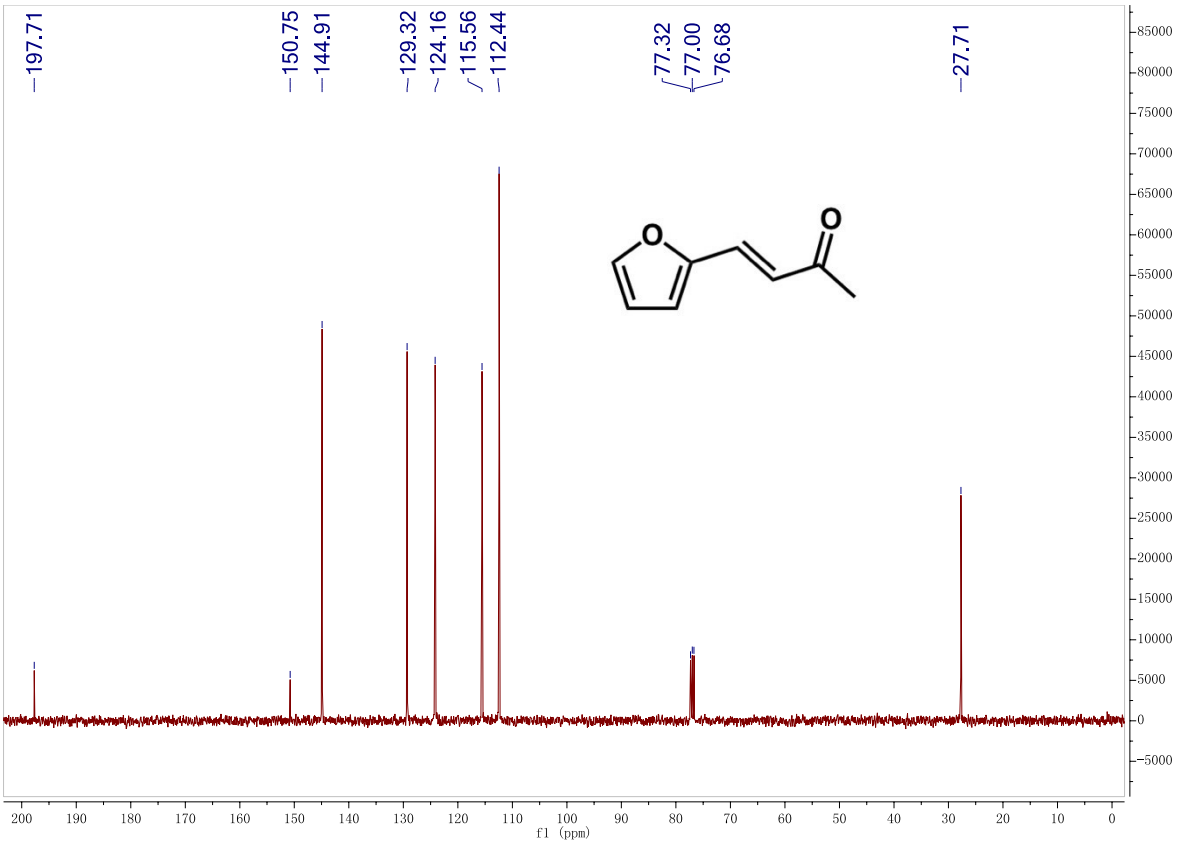

^{1}H-NMR and ^{13}C-NMR spectra of compounds

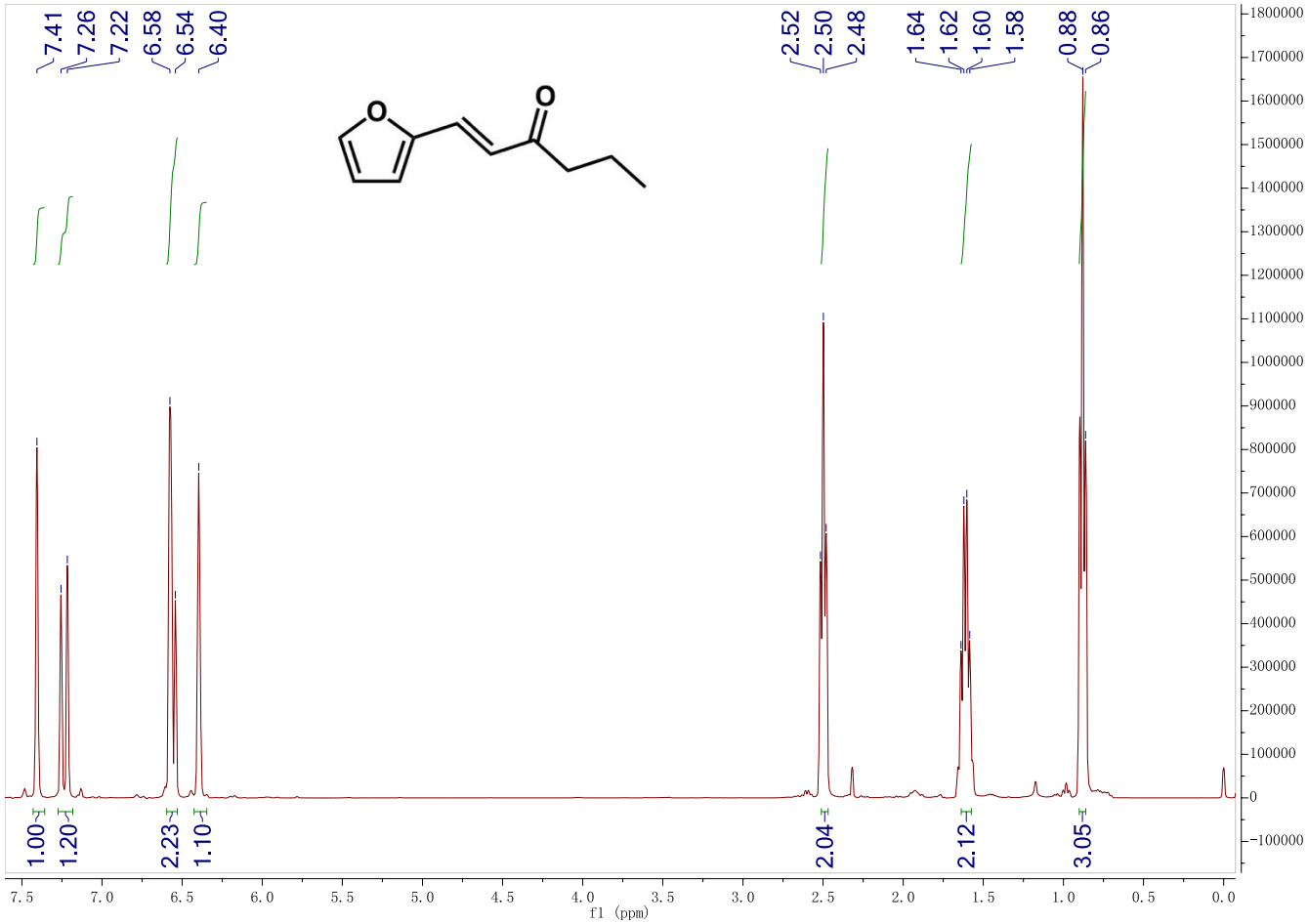
7.41
7.26
7.22
6.58
6.54
6.40
2.52
2.50
2.48
1.64
1.62
1.60
1.58
0.88
0.86
1.00
1.20
2.23
1.10
2.04
2.12
3.05
f1 (ppm)

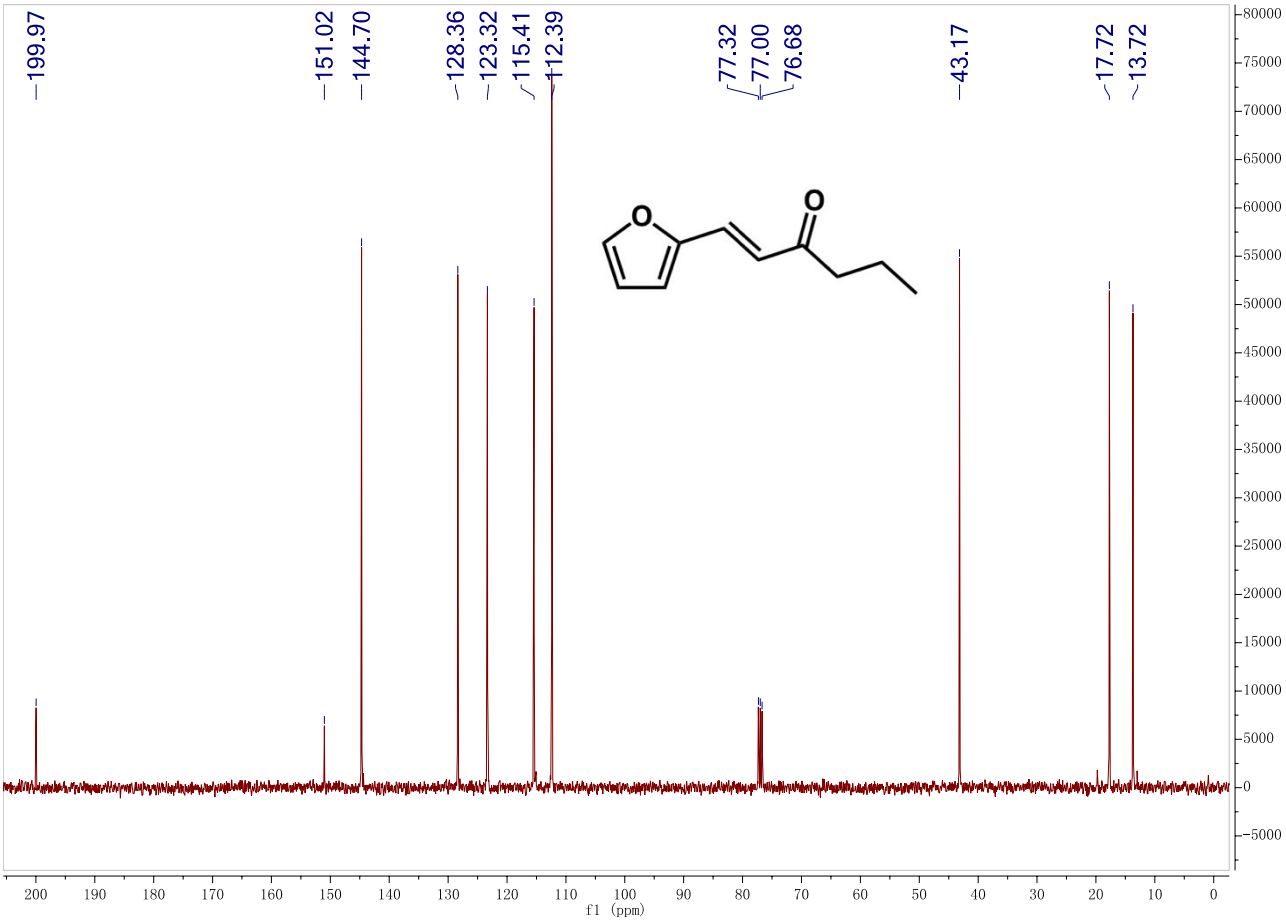
199.97
151.02
144.70
128.36
123.32
115.41
112.39
77.32
77.00
76.68
43.17
17.72
13.72
f1 (ppm)

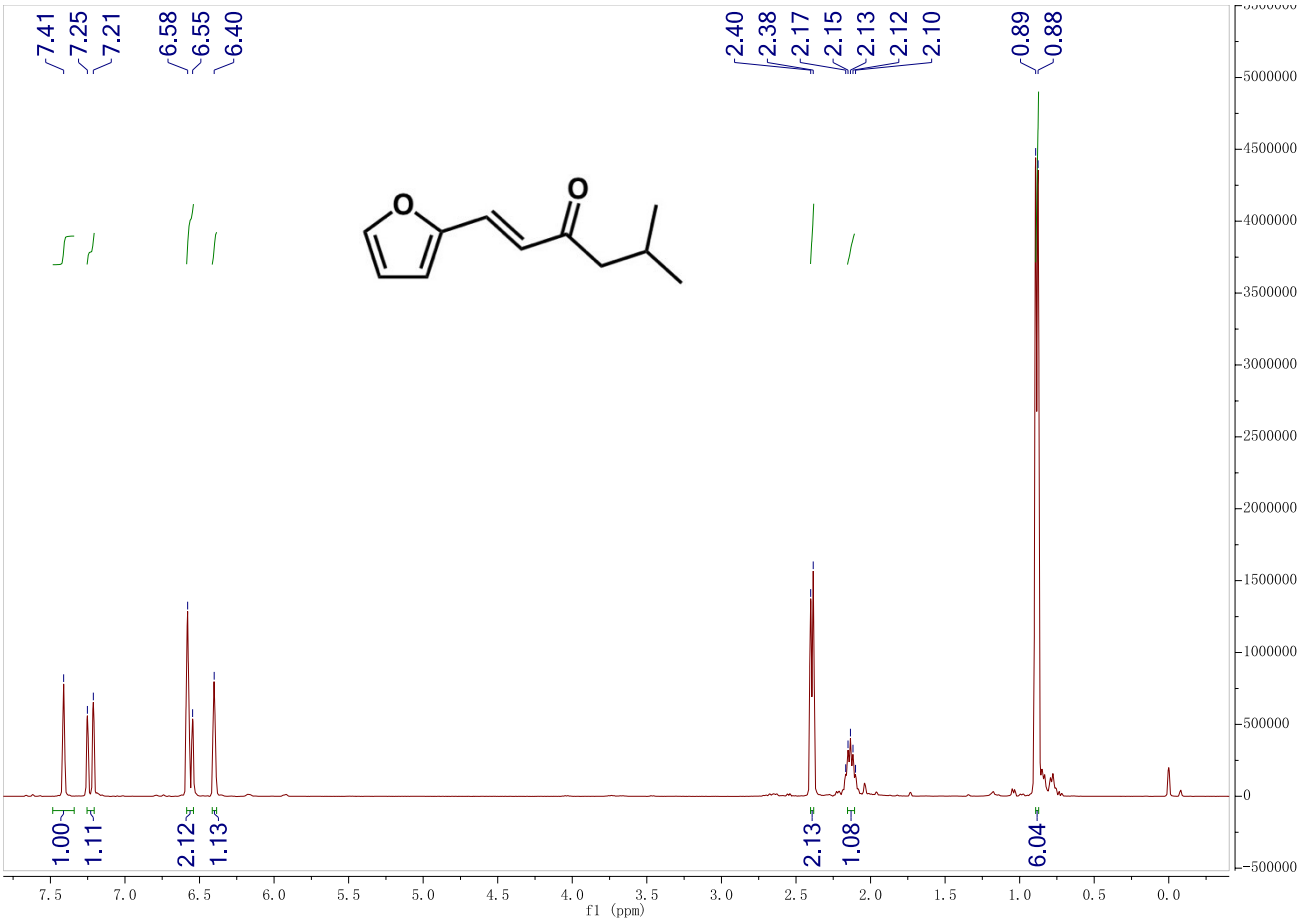
7.41
7.25
7.21
6.58
6.55
6.40
2.40
2.38
2.17
2.15
2.13
2.12
2.10
0.89
0.88
1.00
1.11
2.12
1.13
2.13
1.08
6.04
f1 (ppm)

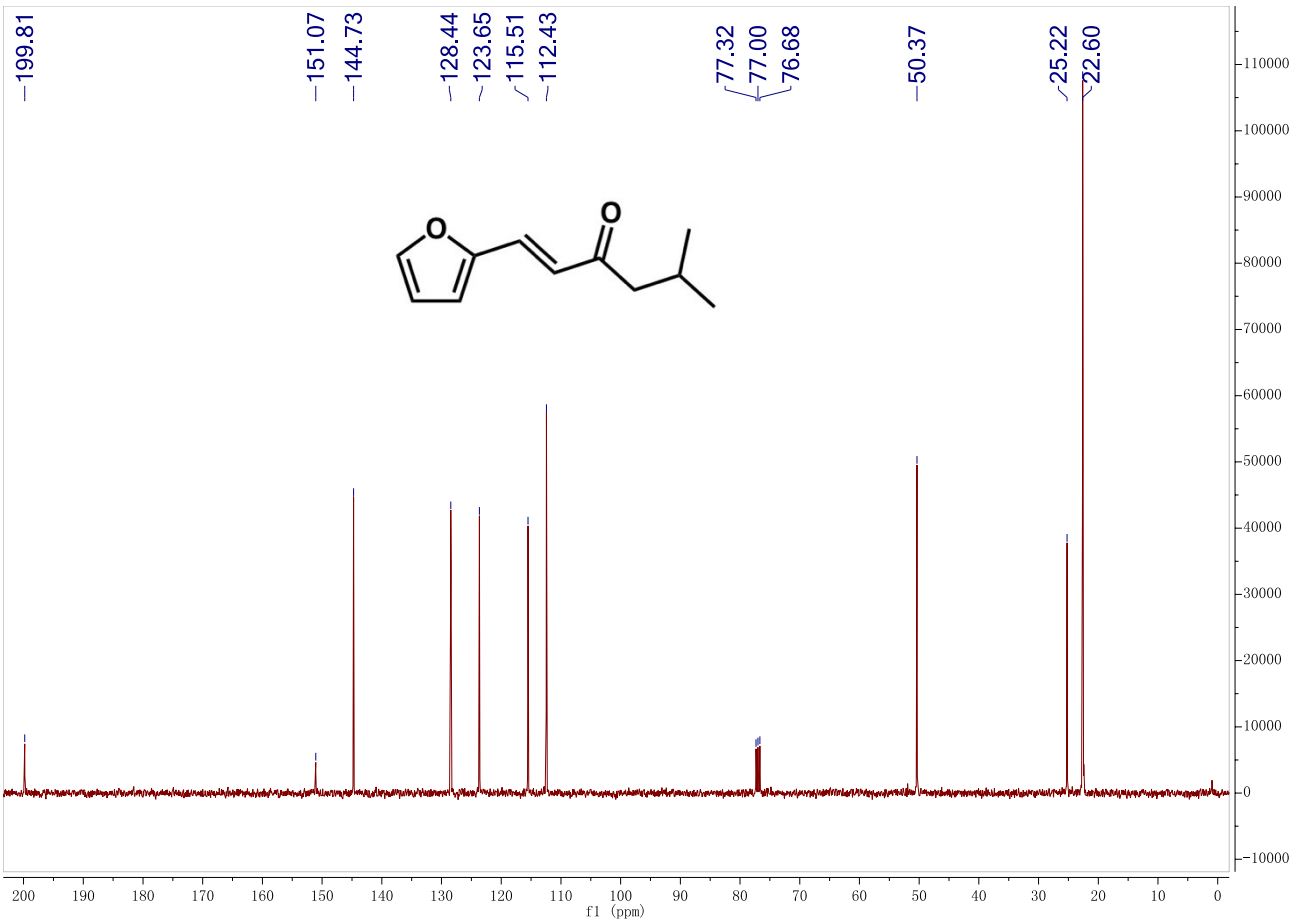
199.81
151.07
144.73
128.44
123.65
115.51
112.43
77.32
77.00
76.68
50.37
25.22
22.60
f1 (ppm)

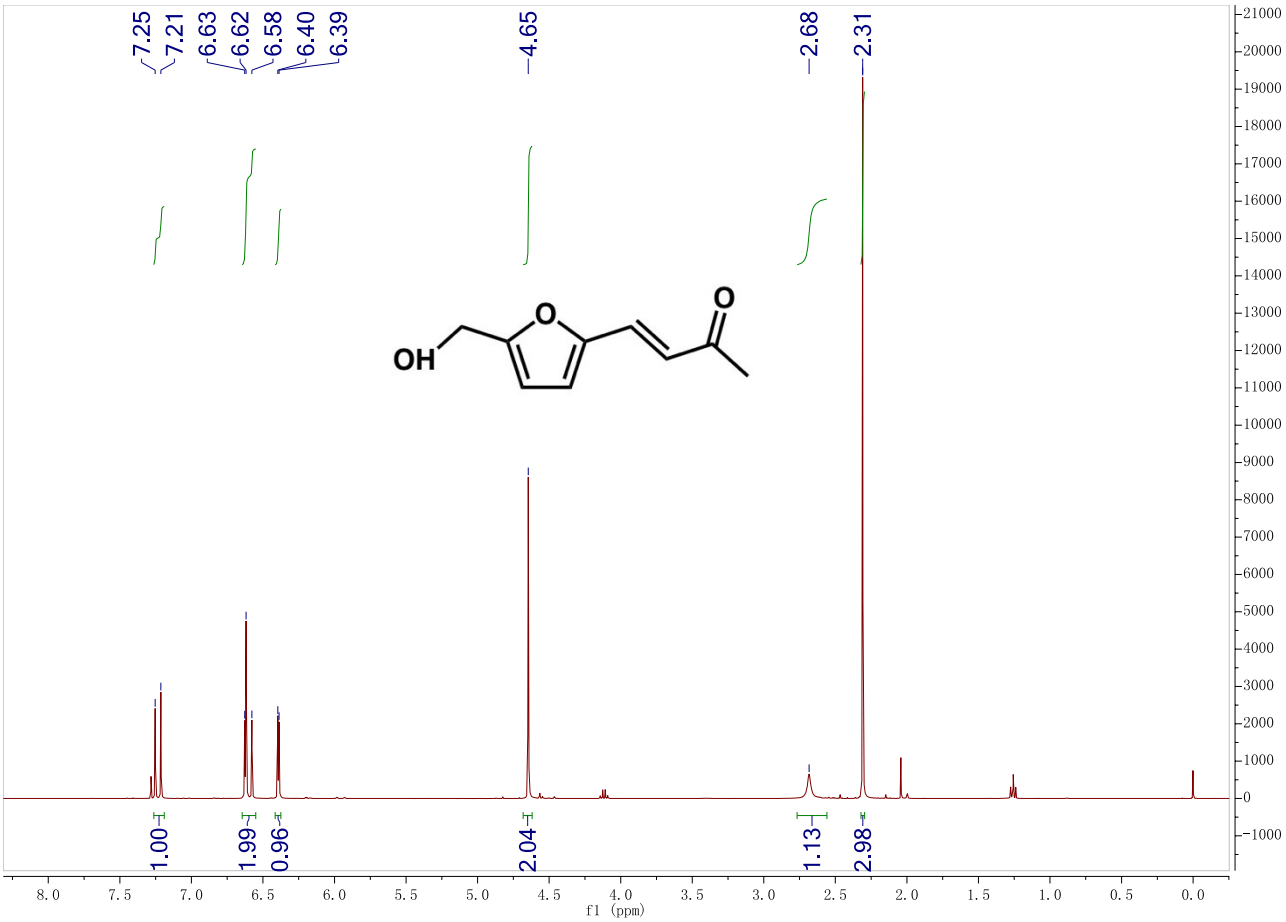
7.25
7.21
6.63
6.62
6.58
6.40
6.39
4.65
2.68
2.31
OH
O
O
1.00
1.99
0.96
2.04
1.13
2.98
f1 (ppm)

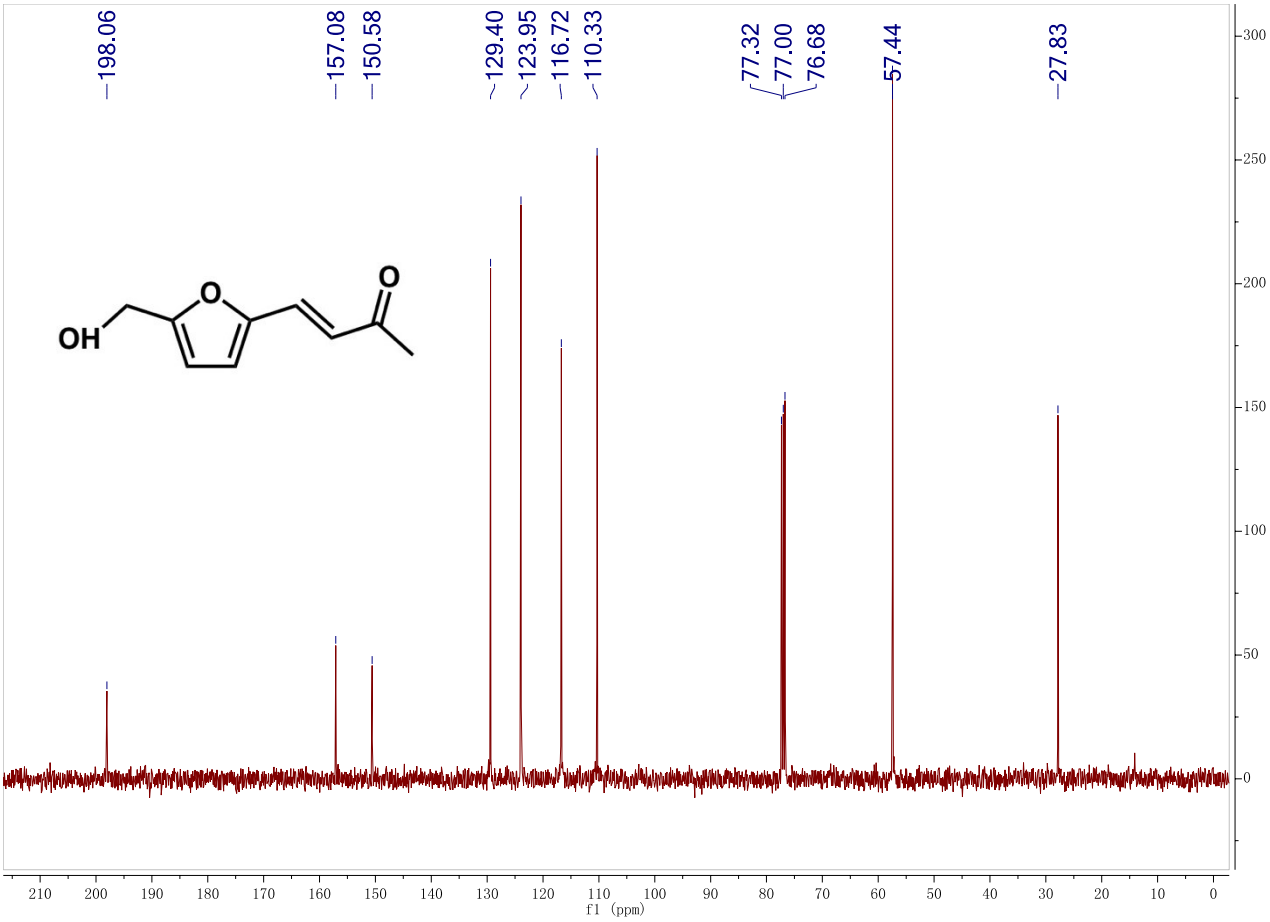
198.06
157.08
150.58
129.40
123.95
116.72
110.33
77.32
77.00
76.68
57.44
27.83
OH
O
O
f1 (ppm)

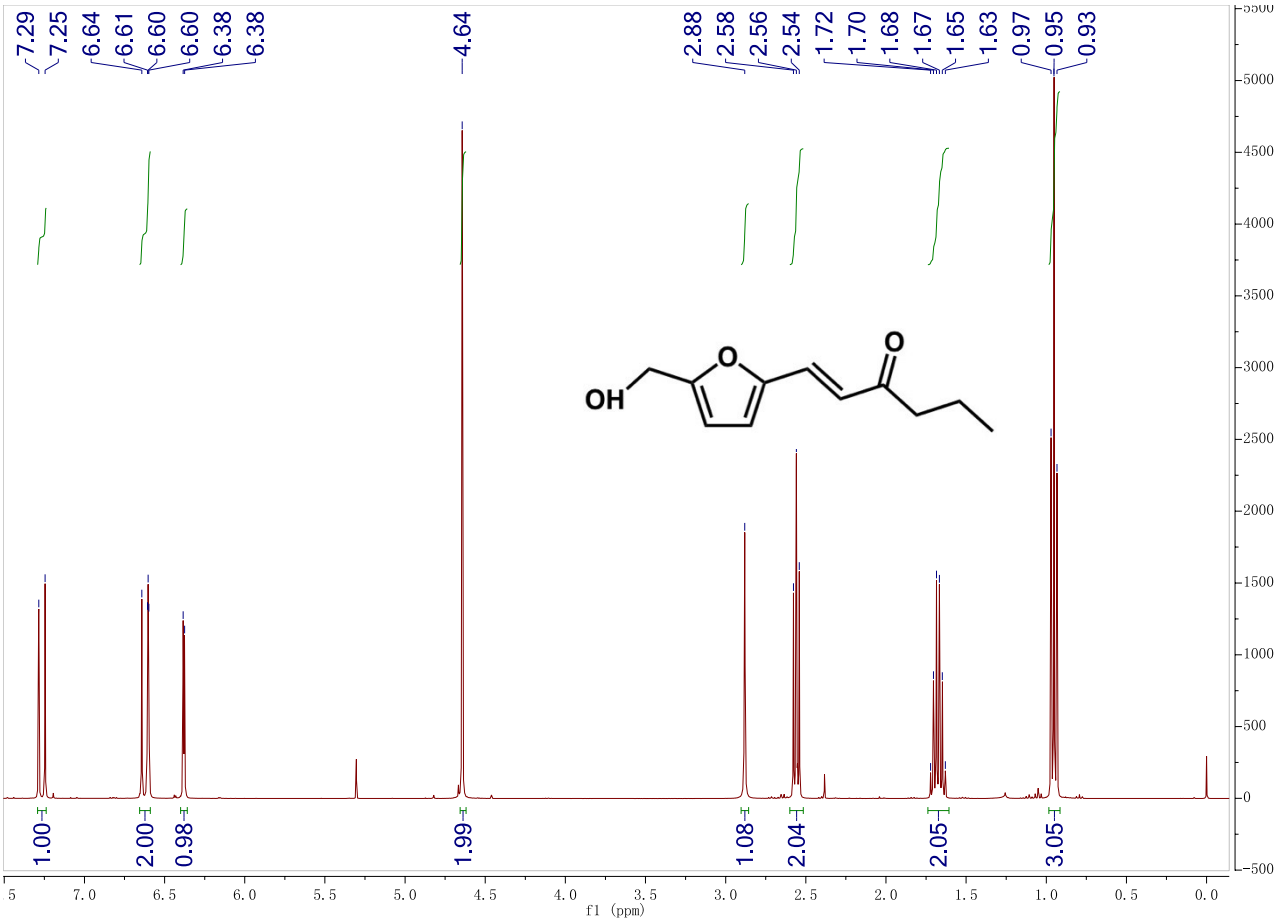
7.29
7.25
6.64
6.61
6.60
6.60
6.38
6.38
4.64
2.88
2.58
2.56
2.54
1.72
1.70
1.68
1.67
1.65
1.63
0.97
0.95
0.93
OH
O
O
1.00
2.00
0.98
1.99
1.08
2.04
2.05
3.05
f1 (ppm)

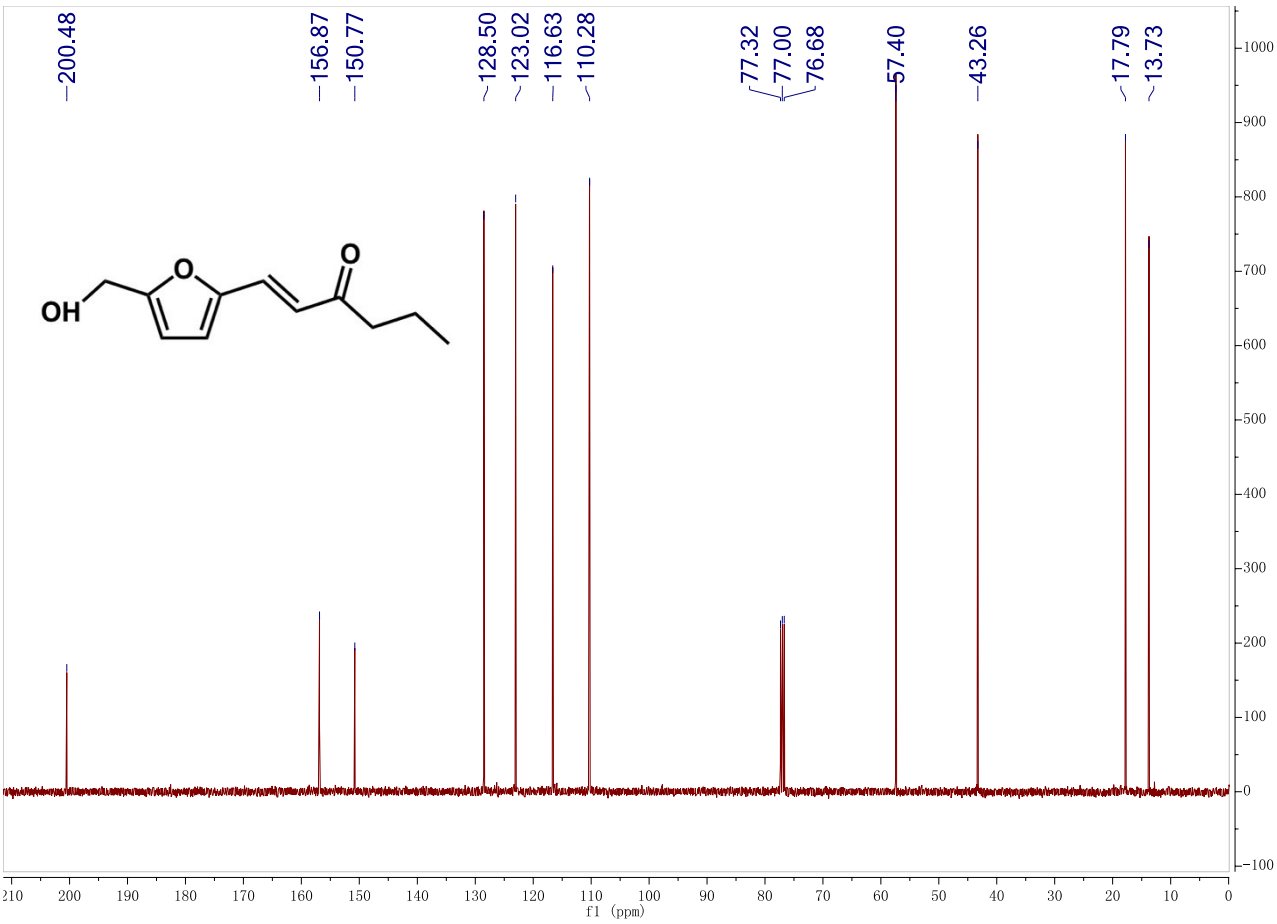
200.48
156.87
150.77
128.50
123.02
116.63
110.28
77.32
77.00
76.68
57.40
43.26
17.79
13.73
OH
O
O
f1 (ppm)

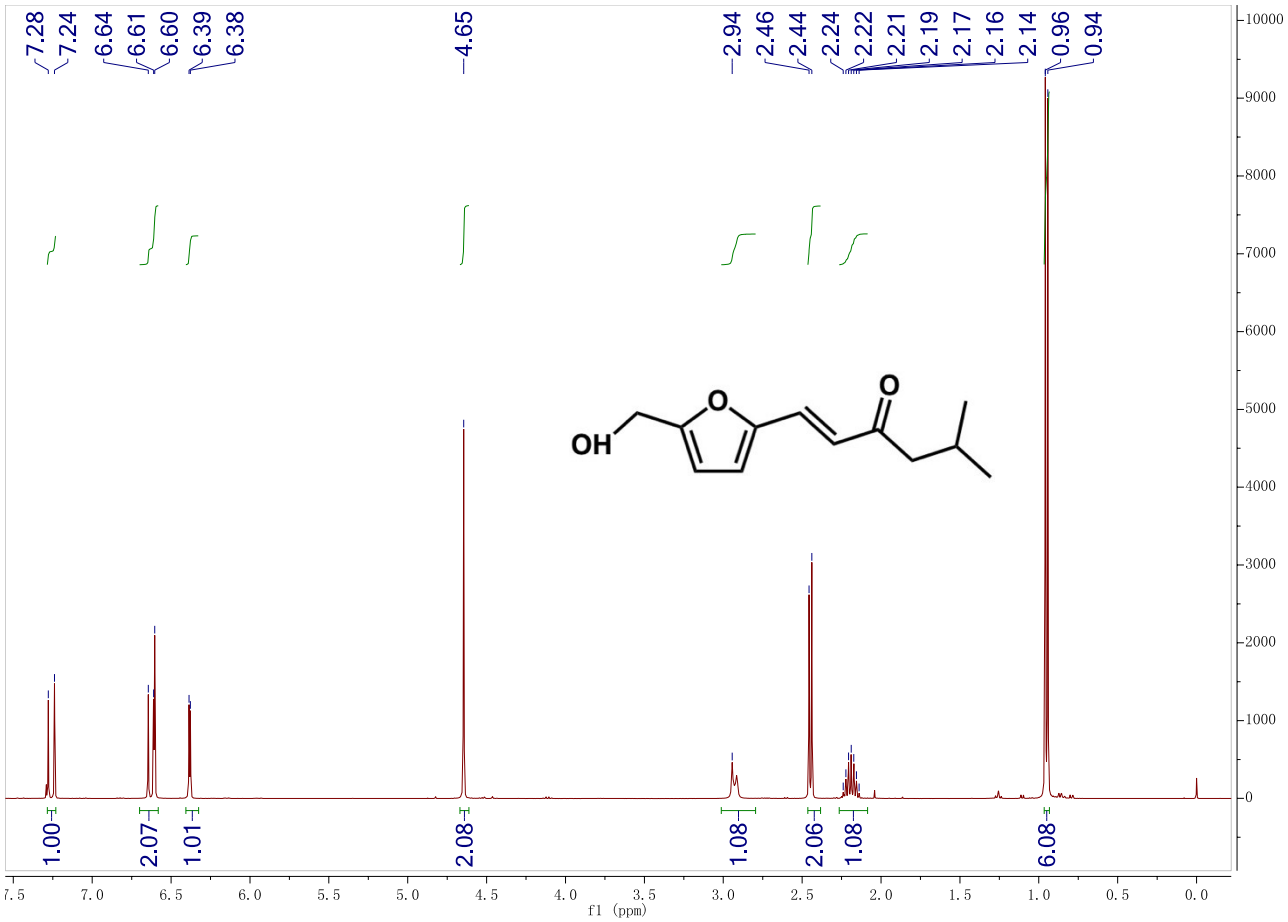
7.28
7.24
6.64
6.61
6.60
6.39
6.38
4.65
2.94
2.46
2.44
2.24
2.22
2.21
2.19
2.17
2.16
2.14
0.96
0.94
OH
O
O
1.00
2.07
1.01
2.08
1.08
2.06
1.08
6.08
f1 (ppm)


200.29
156.91
150.78
128.57
123.31
116.72
110.30
77.32
77.00
76.68
57.40
50.41
25.29
22.58
OH
O
O
f1 (ppm)

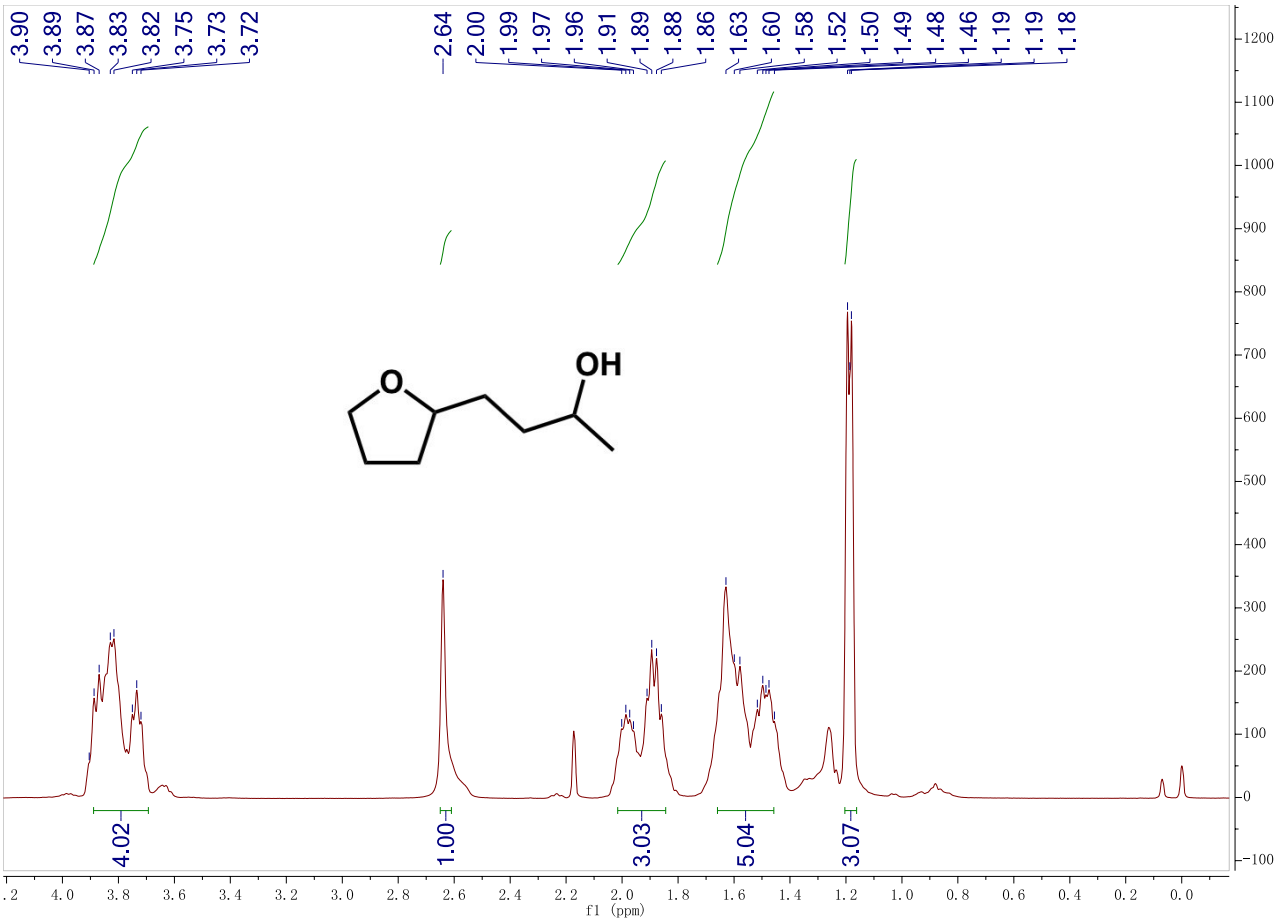
3.90
3.89
3.87
3.83
3.82
3.75
3.73
3.72
2.64
2.00
1.99
1.97
1.96
1.91
1.89
1.88
1.86
1.63
1.60
1.58
1.52
1.50
1.49
1.48
1.46
1.19
1.19
1.18
O
OH
4.02
1.00
3.03
5.04
3.07
f1 (ppm)

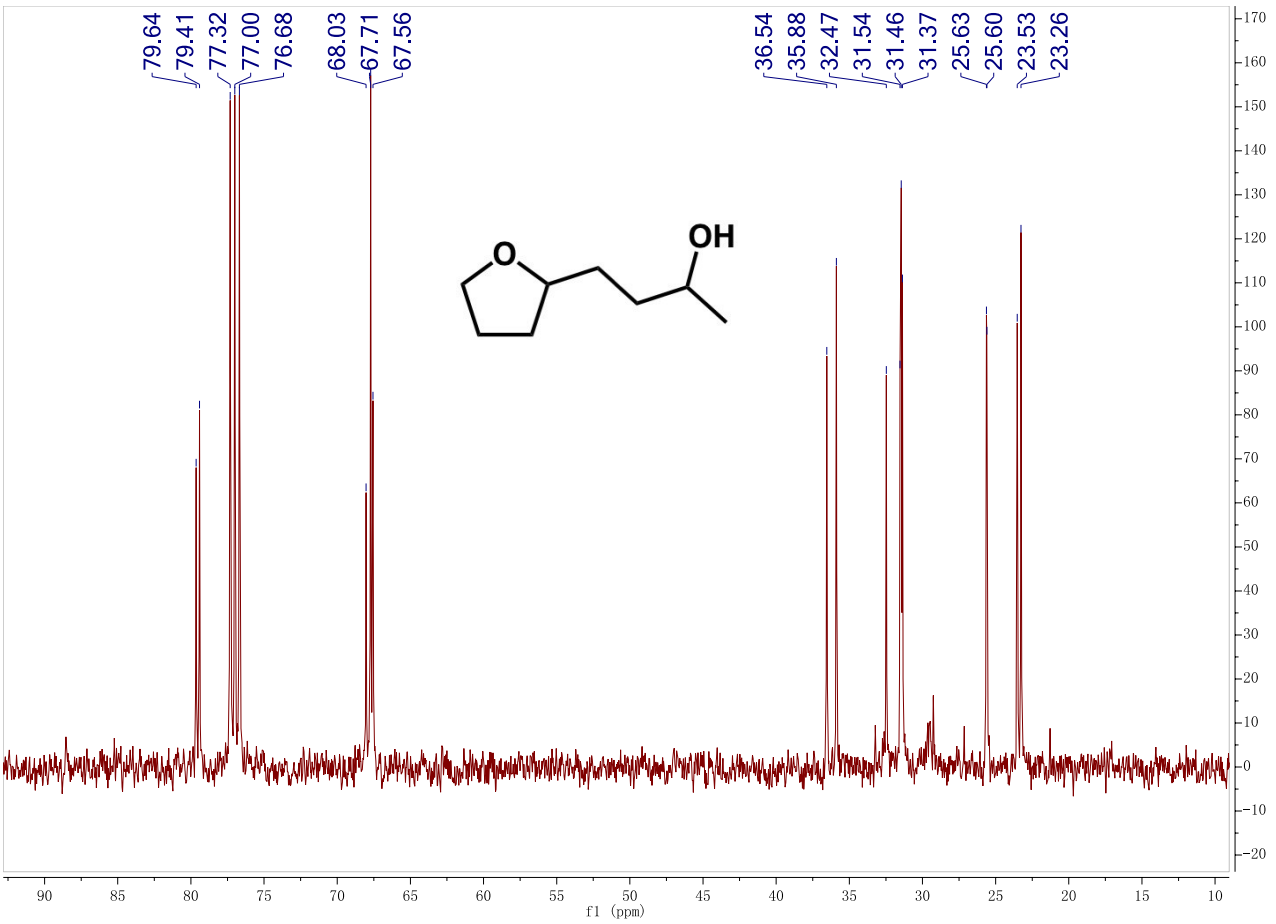
79.64
79.41
77.32
77.00
76.68
68.03
67.71
67.56
36.54
35.88
32.47
31.54
31.46
31.37
25.63
25.60
23.53
23.26
O
OH
f1 (ppm)

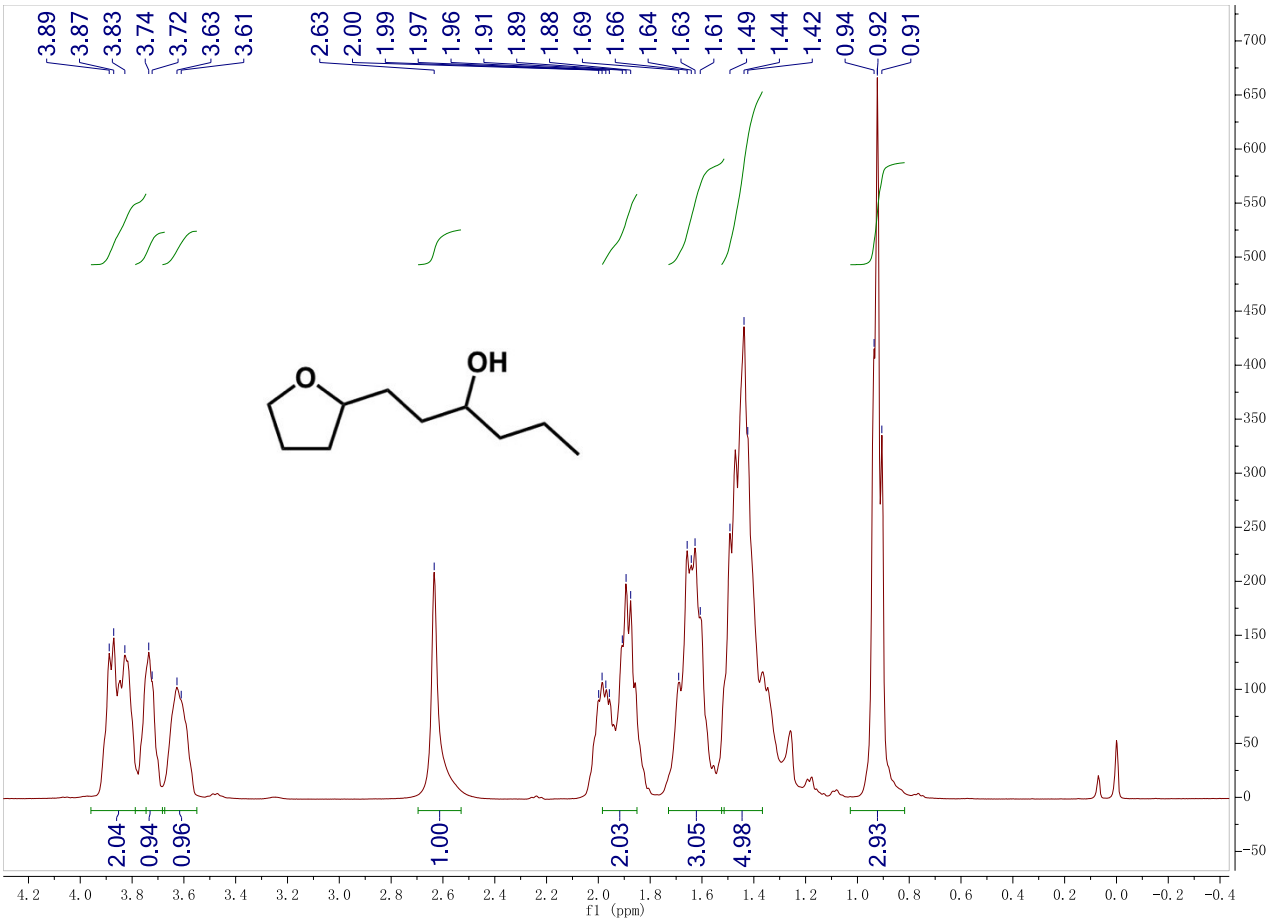
3.89
3.87
3.83
3.74
3.72
3.63
3.61
2.63
2.00
1.99
1.97
1.96
1.91
1.89
1.88
1.69
1.66
1.64
1.63
1.61
1.49
1.44
1.42
0.94
0.92
0.91
OH
O
2.04
0.94
0.96
1.00
2.03
3.05
4.98
2.93
f1 (ppm)

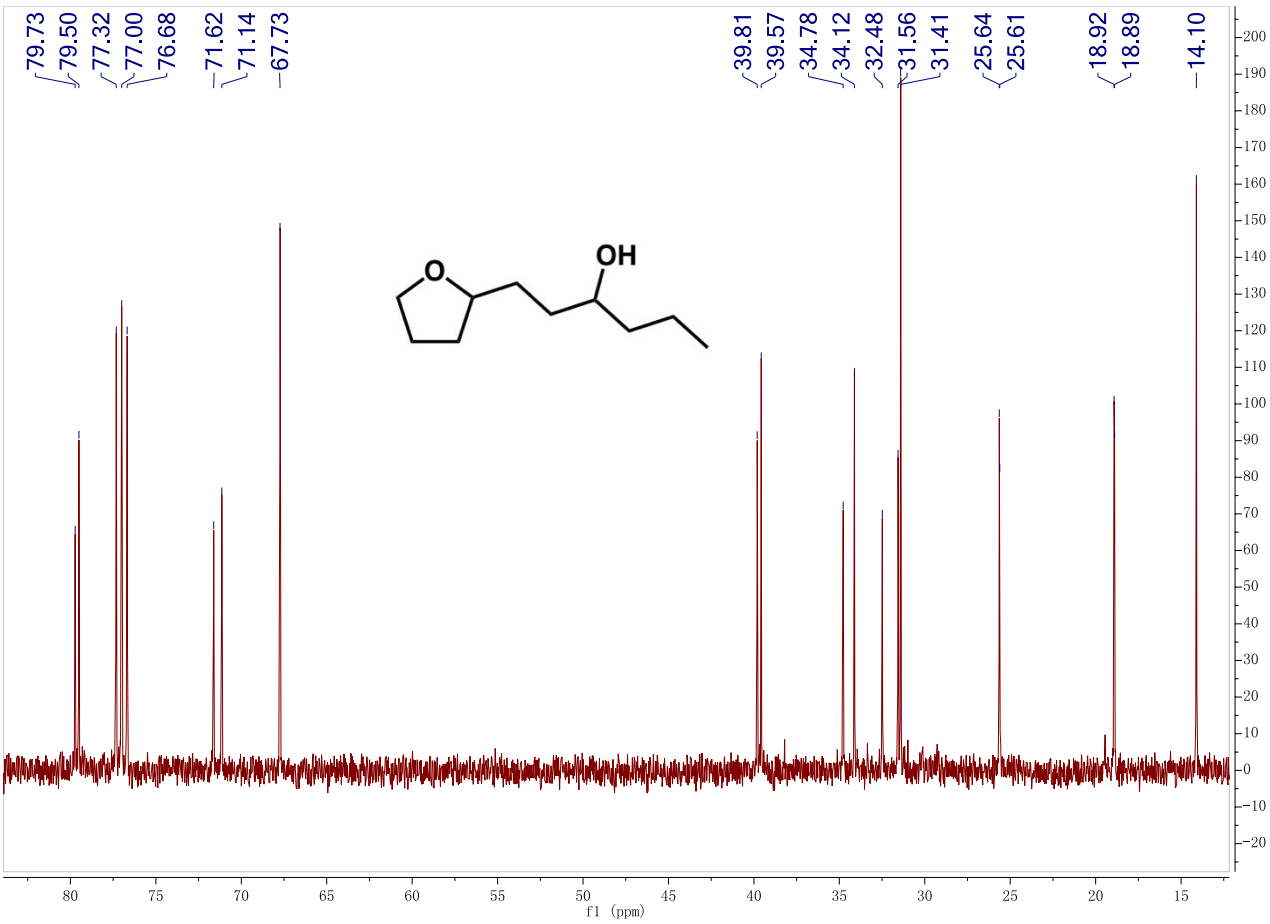
79.73
79.50
77.32
77.00
76.68
71.62
71.14
67.73
39.81
39.57
34.78
34.12
32.48
31.56
31.41
25.64
25.61
18.92
18.89
14.10
OH
O
f1 (ppm)

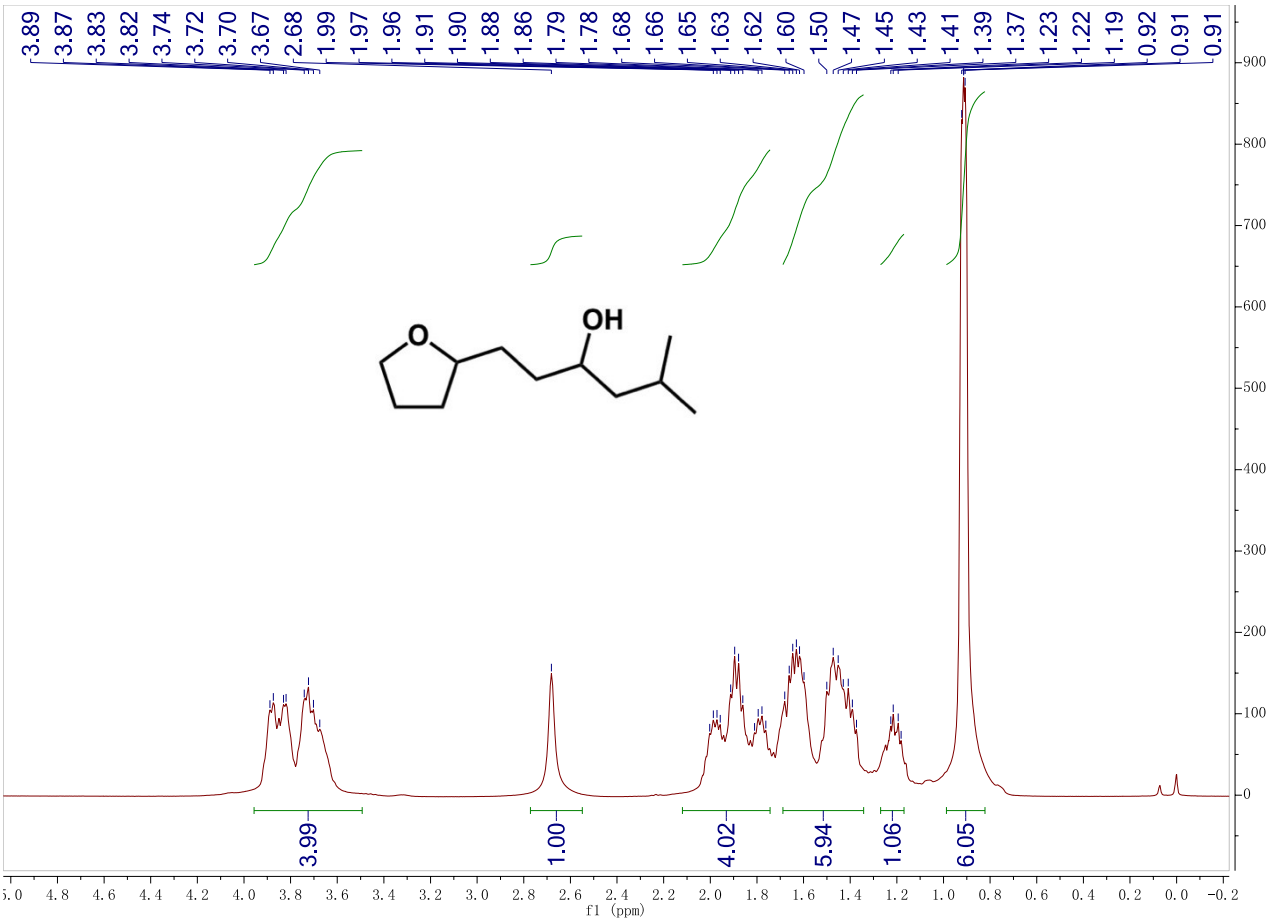
3.89
3.87
3.83
3.82
3.74
3.72
3.70
3.67
2.68
1.99
1.97
1.96
1.91
1.90
1.88
1.86
1.79
1.78
1.68
1.66
1.65
1.63
1.62
1.60
1.50
1.47
1.45
1.43
1.41
1.39
1.37
1.23
1.22
1.19
0.92
0.91
0.91
O
OH
3.99
1.00
4.02
5.94
1.06
6.05
f1 (ppm)

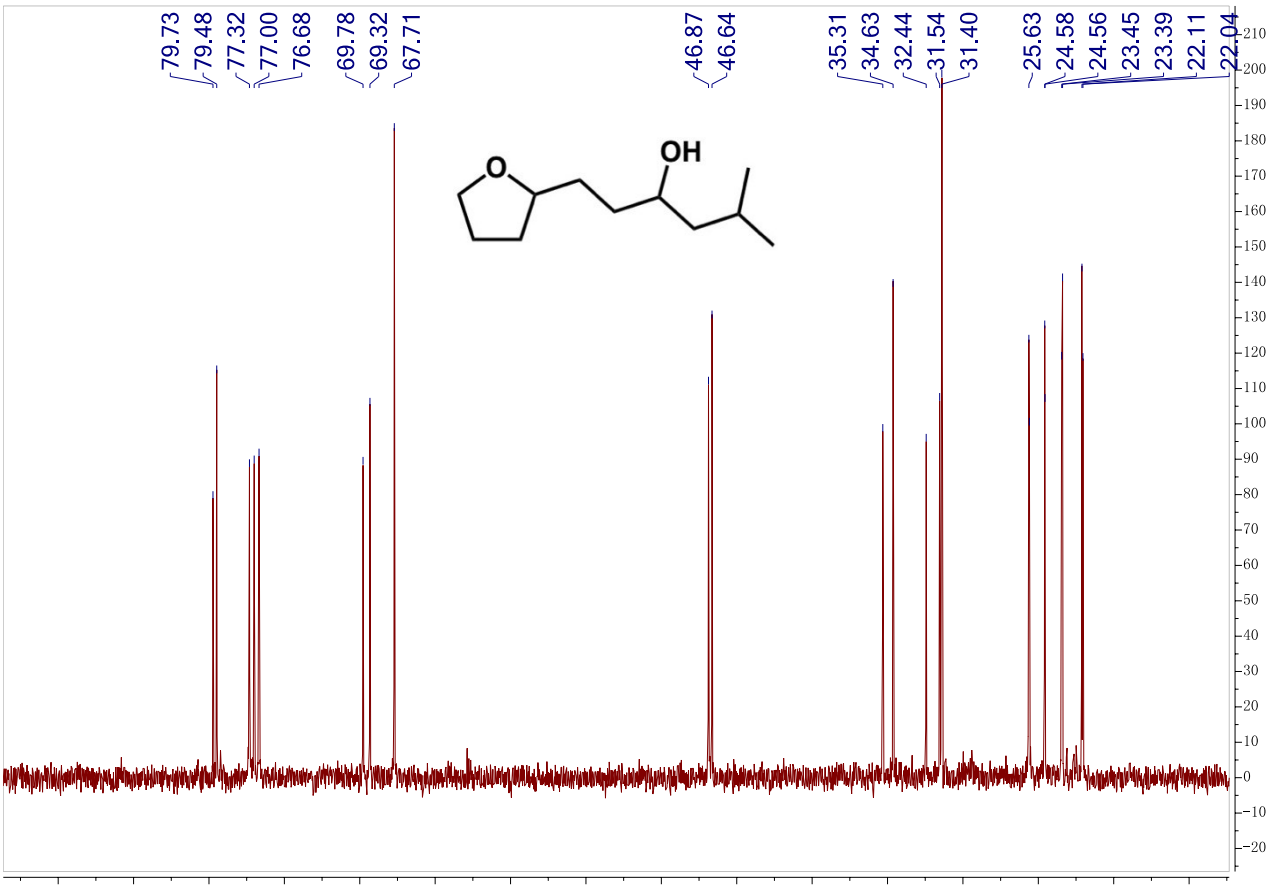
79.73
79.48
77.32
77.00
76.68
69.78
69.32
67.71
46.87
46.64
35.31
34.63
32.44
31.54
31.40
25.63
24.58
24.56
23.45
23.39
22.11
22.04
O
OH

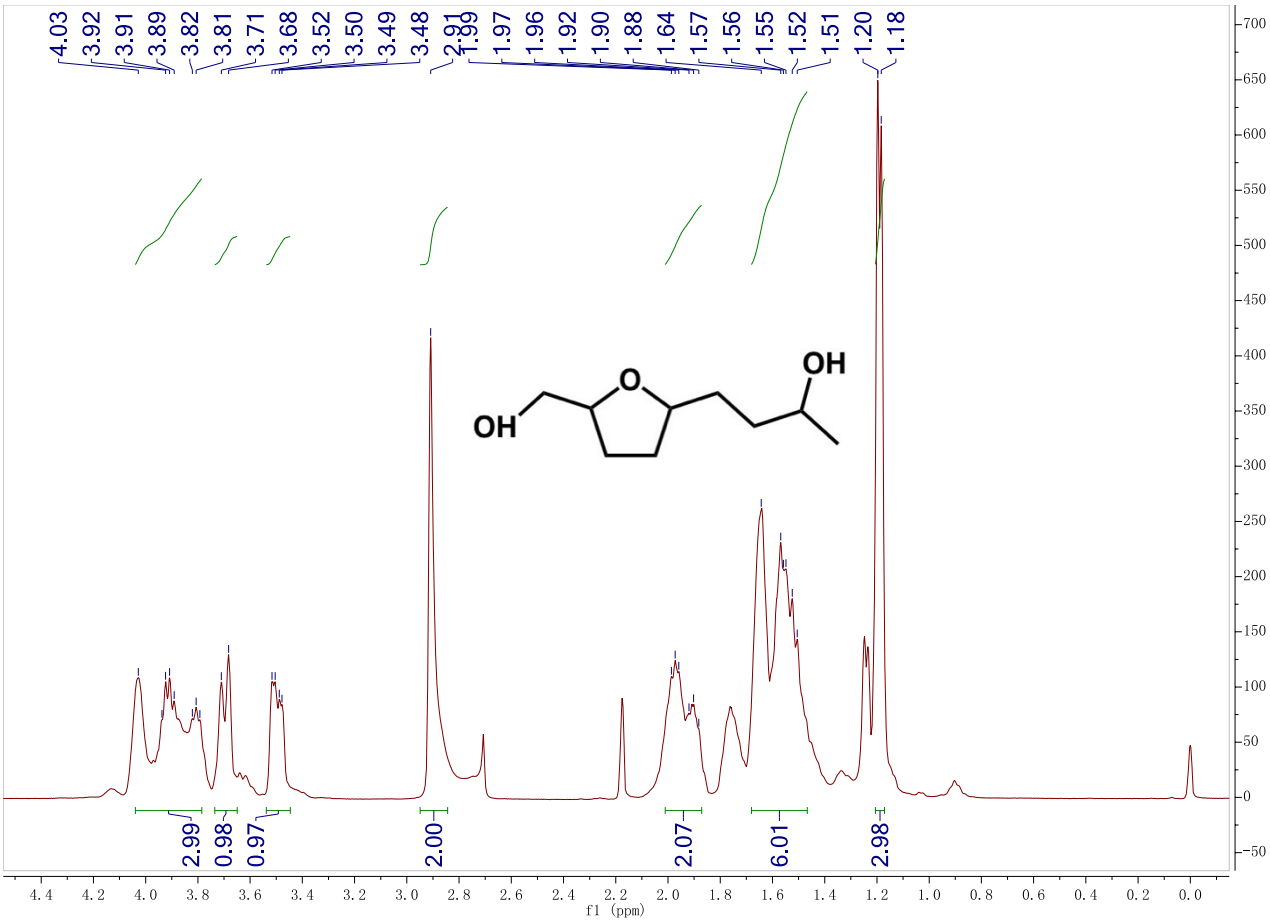
4.03
3.92
3.91
3.89
3.82
3.81
3.71
3.68
3.52
3.50
3.49
3.48
2.91
1.99
1.97
1.96
1.92
1.90
1.88
1.64
1.57
1.56
1.55
1.52
1.51
1.20
1.18
OH
O
OH
2.99
0.98
0.97
2.00
2.07
6.01
2.98
f1 (ppm)

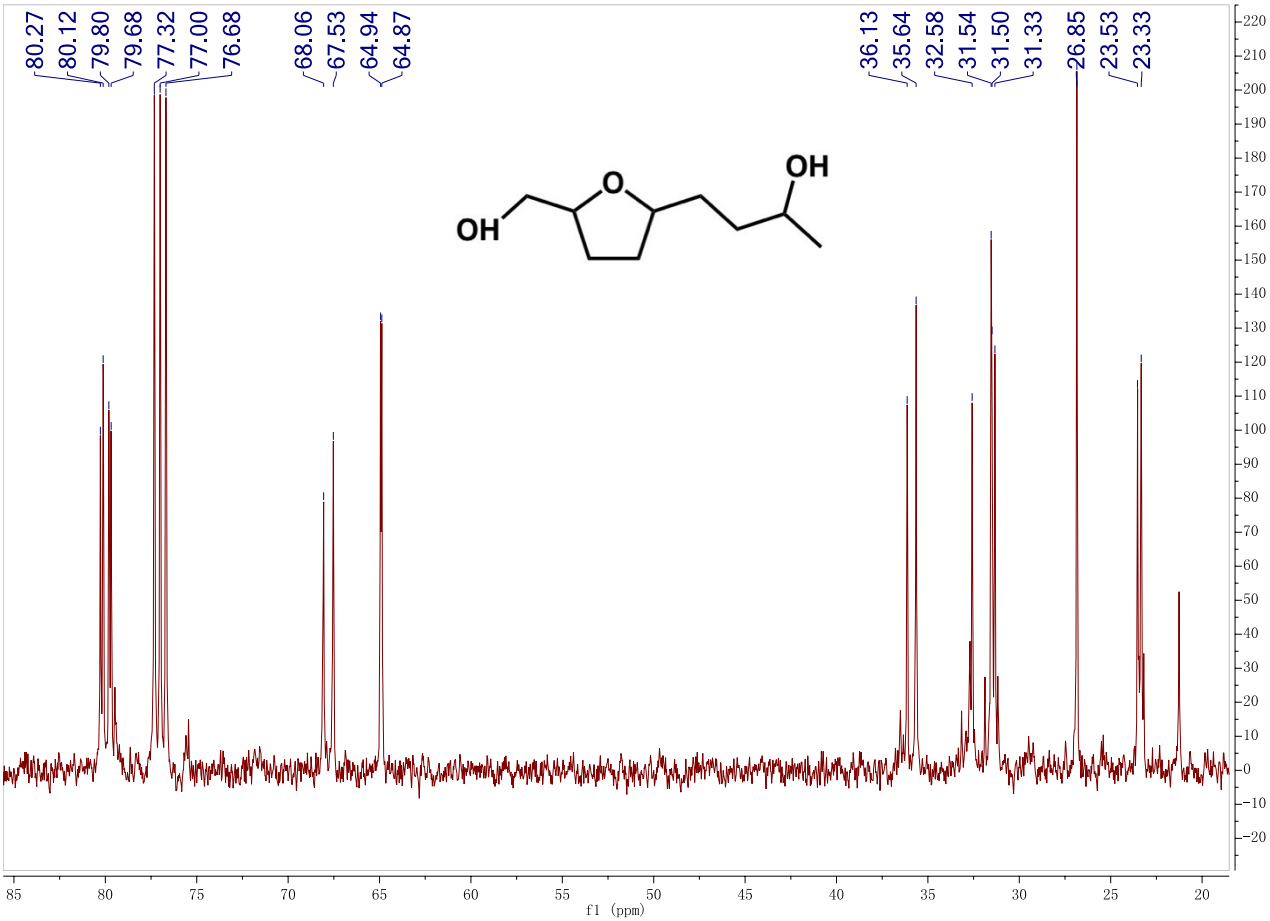
80.27
80.12
79.80
79.68
77.32
77.00
76.68
68.06
67.53
64.94
64.87
36.13
35.64
32.58
31.54
31.50
31.33
26.85
23.53
23.33
OH
O
OH
f1 (ppm)

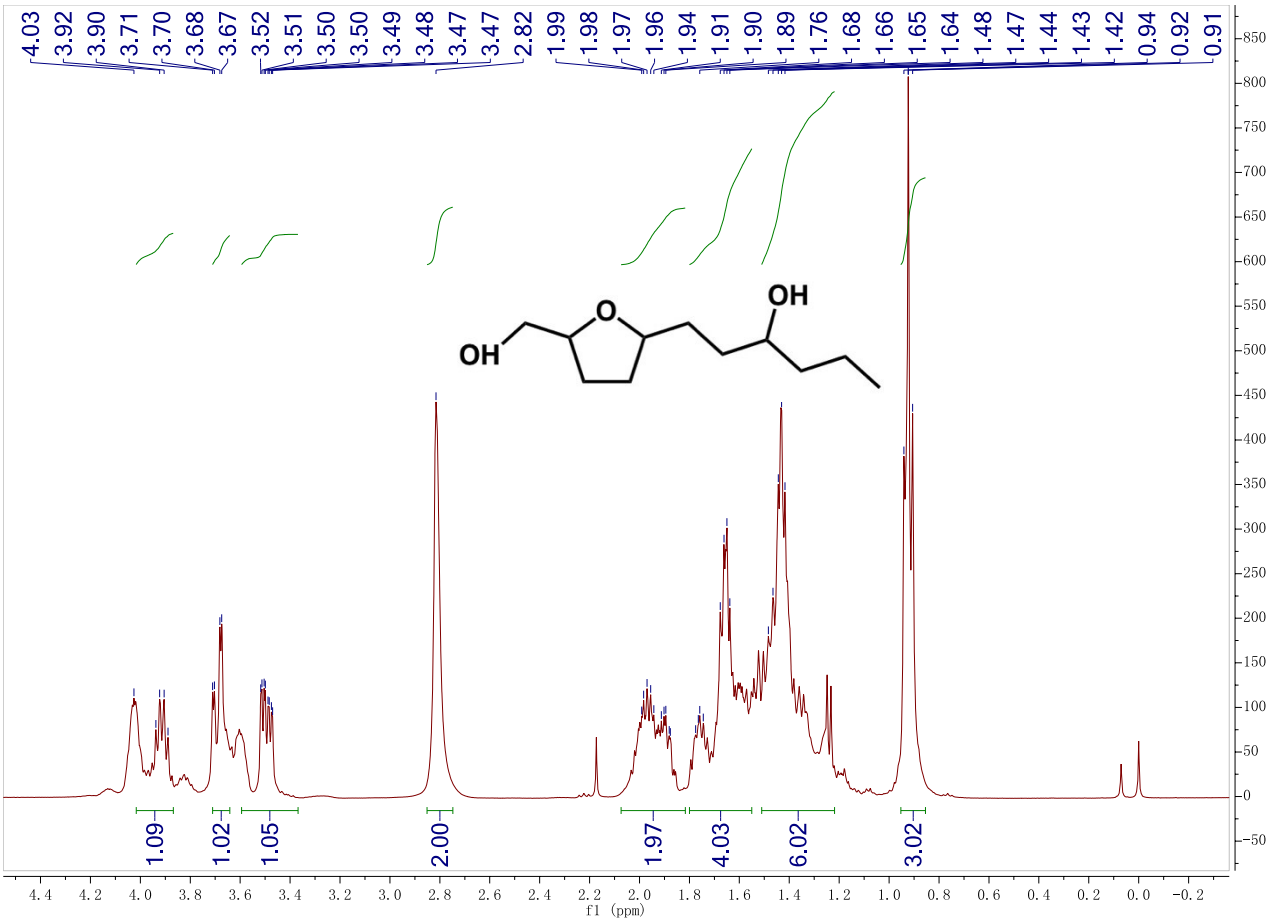
4.03
3.92
3.90
3.71
3.70
3.68
3.67
3.52
3.51
3.50
3.50
3.49
3.48
3.47
3.47
2.82
1.99
1.98
1.97
1.96
1.94
1.91
1.90
1.89
1.76
1.68
1.66
1.65
1.64
1.48
1.47
1.44
1.43
1.42
0.94
0.92
0.91
OH
O
OH
1.09
1.02
1.05
2.00
1.97
4.03
6.02
3.02
f1 (ppm)

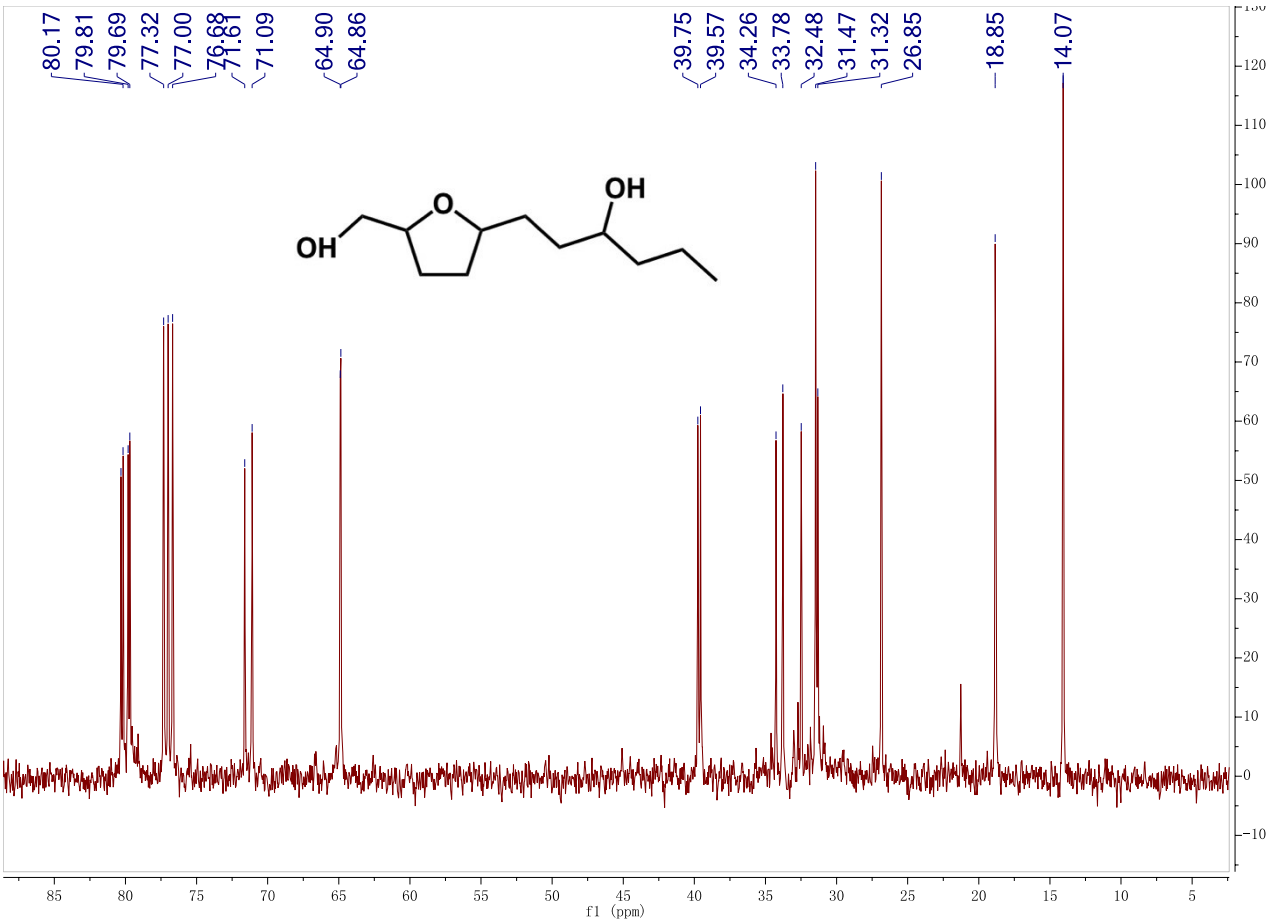
80.17
79.81
79.69
77.32
77.00
76.68
71.61
71.09
64.90
64.86
39.75
39.57
34.26
33.78
32.48
31.47
31.32
26.85
18.85
14.07
OH
O
OH
f1 (ppm)

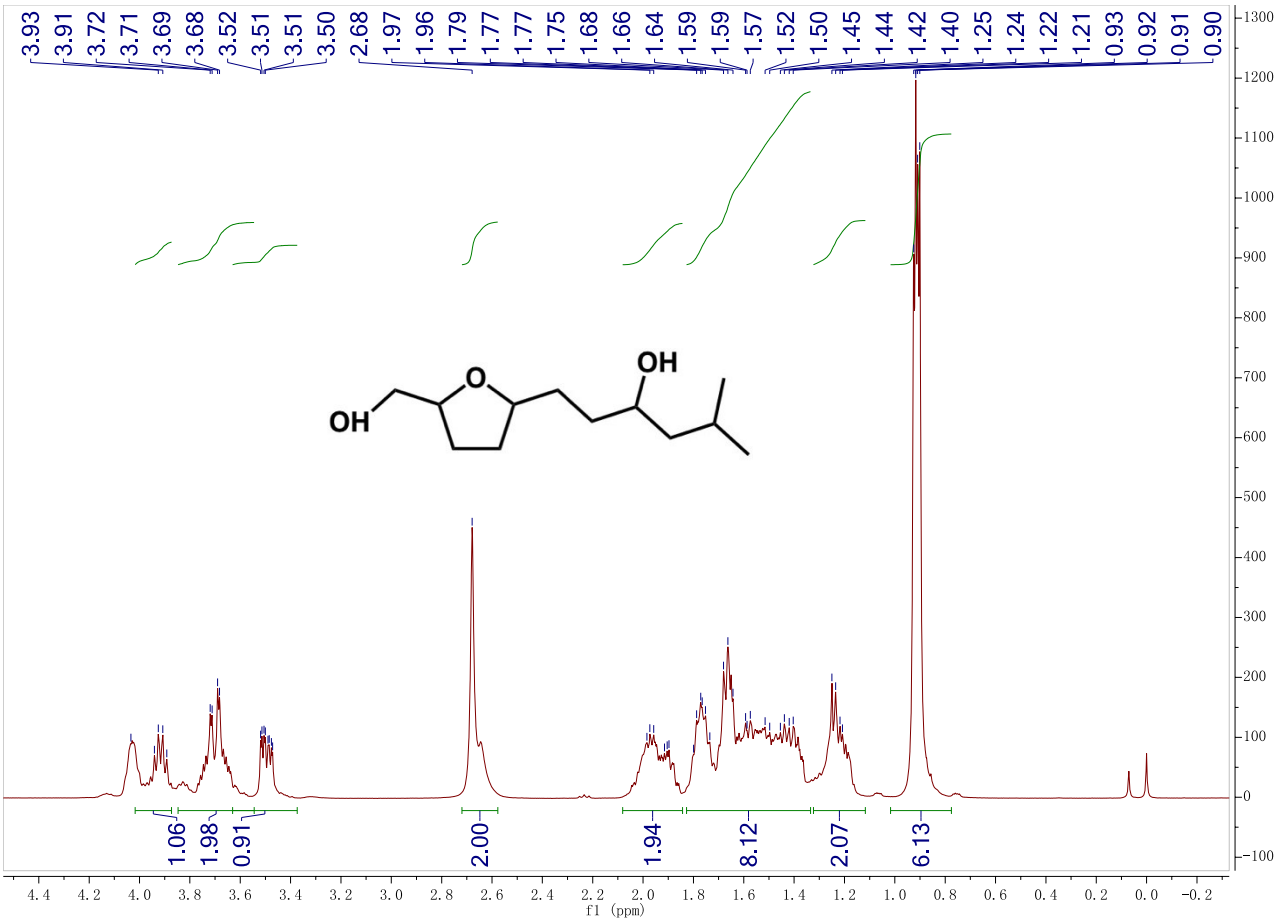
3.93 3.91 3.72 3.71 3.69 3.68 3.52 3.51 3.51 3.50 2.68 1.97 1.96 1.79 1.77 1.77 1.75 1.68 1.66 1.64 1.59 1.59 1.57 1.52 1.50 1.45 1.44 1.42 1.40 1.25 1.24 1.22 1.21 0.93 0.92 0.91 0.90
OH
O
OH
1.06 1.98 0.91 2.00 1.94 8.12 2.07 6.13
f1 (ppm)

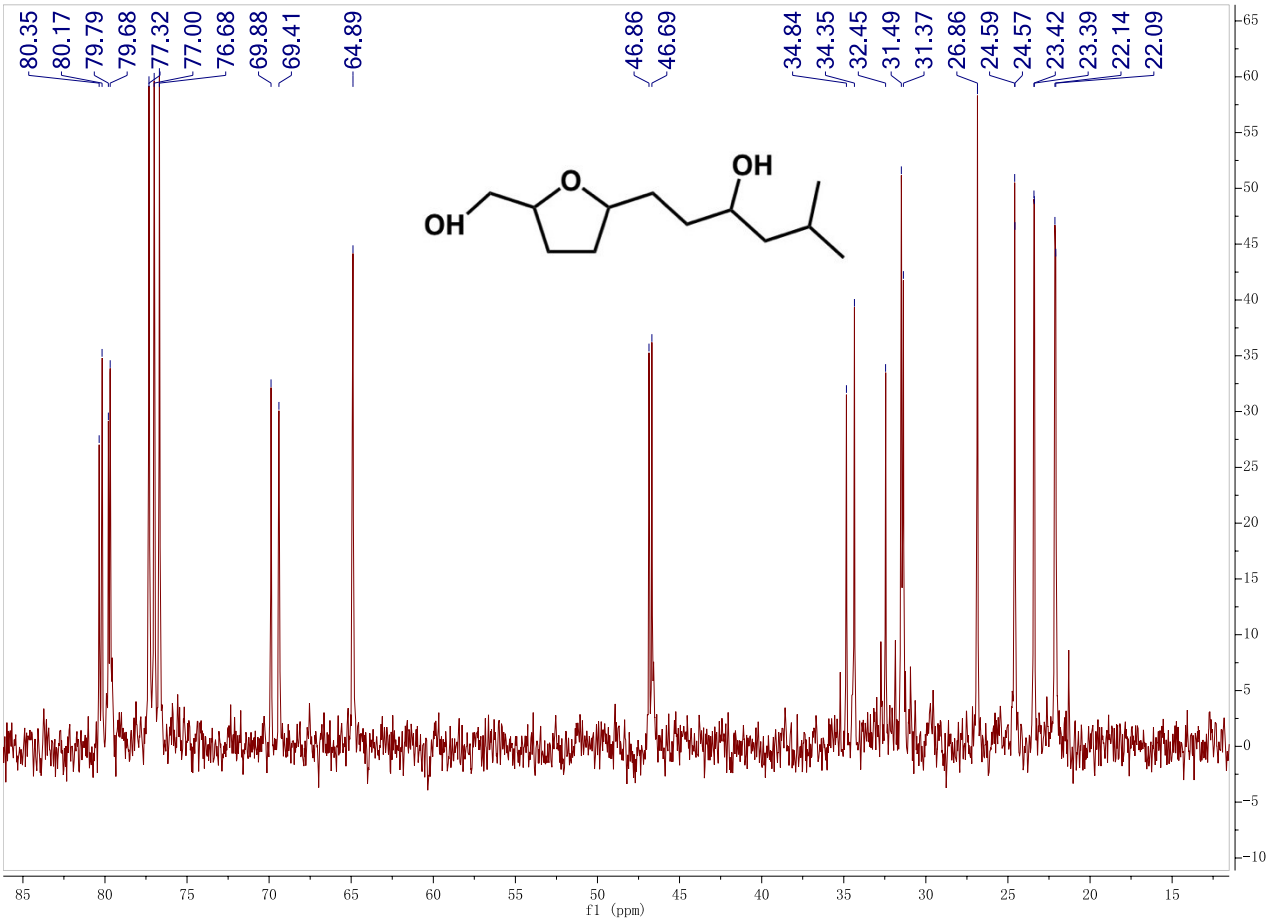
80.35 80.17 79.79 79.68 77.32 77.00 76.68 69.88 69.41 64.89 46.86 46.69 34.84 34.35 32.45 31.49 31.37 26.86 24.59 24.57 23.42 23.39 22.14 22.09
OH
O
OH
f1 (ppm)

Reference:

[S1] S. S. Li, F. Chen, N. Li, W. T. Zhang, X. R. Sheng, A. Q. Wang, Y. Cong, X. D. Wang and T. Zhang, *ChemsusChem,* 2017, **10**, 711−719.

[S2] J. L. Gomez de la Fuente, F.J. Perez-Alonso, M.V. Martınez-Huerta, M.A. Pena, J.L.G. Fierro and S. Rojas, *Catal. Today*, 2009, **143**, 69−75.

[S3] Y. Nakagawa, K. Takada, M. Tamura and K. Tomishige, *Acs Catal.,* 2014, **4**, 2718−2726.

[S4] Y. Nakagawa and K. Tomishige, *Catal. Commun.,* 2010, **12**, 154−156.

[S5] B. F. Chen, F. B. Li, Z. J. Huang and G. Q. Yuan, *Appl. Catal. A: Gen.,* 2015, **500**, 23−29.

[S6] M. Lesiak, M. Binczarski, S. Karski, W. Maniukiewicz, J. Rogowski, E. Szubiakiewicz, J. Berlowska, P. Dziugan and I. Witonska, *J. Mol. Catal. A: Chem.,* 2014, **395**, 337−348.

[S7] S. Bhogeswararao and D. Srinivas, *J. Catal.,* 2015, **327**, 65−77.

[S8] N. S. Biradar, A. M. Hengne, S. N. Birajdar, P. S. Niphadkar, P. N. Joshi, and C. V. Rode, *ACS Sustain. Chem. Eng.,* 2014, **2**, 272−281.

[S9] C. Li, G. Y. Xu, X. H. Liu, Y. Zhang and Y. Fu, *Ind. Eng. Chem. Res.*, 2017, **56**, 8843−8849.

[S10] R. Albilali, M. Douthwaite, Q. He and S. H. Taylor, *Catal. Sci. Technol.*, 2018, **8**, 252−267.

[S11] R. J. Huang, Q. Q. Cui, Q. Q. Yuan, H. H. Wu, Y. J. Guan and P. Wu, *ACS Sustain. Chem. Eng.*, 2018, **6**, 6957−6964.

[S12] L. J. Liu, H. Lou and M. Chen, *Int. J. Hydrogen Energy,* 2016, **41**, 14721−14731.

[S13] J. Wu, G. Gao, J. L. Li, P. Sun, X. D. Long and F. W. Li, *Appl. Catal. B: Environ.,* 2017, **203**, 227−236.

[S14] Y. L. Yang, J. P. Ma, X. Q. Jia, Z. T. Du, Y. Duan and J. Xu, *RSC Adv.,* 2016, **6**, 51221−51228.

[S15] Y. P. Su, C. Chen, X. G. Zhu, Y. Zhang, W. B. Gong, H. M. Zhang, H. J. Zhao and G. Z. Wang, *Dalton Trans.*, 2017, **46**, 6358−6365.

[S16] W. B. Gong, C. Chen, H. M. Zhang, Y. Zhang, Y. X. Zhang, G. Z. Wang and H. J. Zhao, *J. Mol. Catal. A: Chem.,* 2017, **429**, 51−59.

[S17] Z. R. Zhang, J. L. Song, Z. W. Jiang, Q. L. Meng, P. Zhang and B. X. Han, *ChemCatChem*, 2017, **9**, 2448−2452.

[S18] J. J. Shi, M. S. Zhao, Y. Y. Wang, J. Fu, X. W. Lu and Z. Y. Hou, *J. Mater. Chem. A.,* 2016, **4**, 5842−5848.

[S19] R. Herbois, S. Noël, B. Léger, S. Tilloy, S. Menuel, A. Addad, B. Martel, A. Ponchel and E. Monflier, *Green Chem.*, 2015, **17**, 2444−2454.

[S20] J. Ftouni, A. Muñoz-Murillo, A. Goryachev, J. P. Hofmann, E. J. M. Hensen, L. Lu, C. J. Kiely, P. C. A. Bruijnincx and B. M. Weckhuysen, *ACS Catal.*, 2016, **6**, 5462−5472.

[S21] K. Gupta and S. K. Singh, *ACS Sustain. Chem. Eng.,* 2018, **6**, 4793−4800.

[S22] J. Julis, M. Hölscher and W. Leitner, *Green Chem.*, 2010, **12**, 1634−1639.